WILEY-VCH

DOI: 10.1002/ ((please add manuscript number))
Article type: Review

Protected Lithium Metal Anode in Batteries: From Liquid to Solid

Chunpeng Yang[†], *Kun (Kelvin) Fu*[†], *Ying Zhang, Emily Hitz, and Liangbing Hu*[*]

Dr. C. Yang, Dr. K. Fu, Y. Zhang, E. Hitz, Dr. L. Hu
Department of Materials Science and Engineering, University of Maryland at College Park, College Park, Maryland 20742, USA
E-mail: binghu@umd.edu
[†] These authors contributed equally to this work.

Keywords: Electrochemical energy storage, Li metal anode, dendrite growth, organic electrolyte, solid-state electrolyte

Abstract:

High-energy lithium metal batteries are among the most promising candidates for next-generation energy storage systems. With a high specific capacity and a low reduction potential, the Li metal anode has attracted extensive interest for decades. Dendritic Li formation, uncontrolled interfacial reactions, and huge volume effect are major hurdles to the commercial application of the Li metal anodes. Recent studies have shown that the performance and safety of Li metal anodes can be significantly improved via organic electrolyte modification, Li metal interface protection, Li electrode framework design, separator coating, and so on. Superior to the liquid electrolytes, solid-state electrolytes are considered able to inhibit problematic Li dendrites and build safe solid Li metal batteries. Inspired the bright prospects of solid Li metal batteries, increasing efforts have been devoted to overcoming the obstacles of solid Li metal batteries, such as low ionic conductivity of the electrolyte, and Li-electrolyte interfacial problems. In this review, the approaches to protect Li metal anodes from liquid batteries to solid-state batteries are outlined and analyzed in detail. Perspectives regarding the strategies for developing Li metal anodes are discussed to facilitate the practical application of the Li metal batteries.

1. Introduction

Efficient and cost-effective batteries have attracted great interest for energy storage. The lithium-ion (Li-ion) battery has gained considerable success during the past decades but its energy density (theoretically ~390 W h kg^{-1}) cannot meet the ever-increasing demands for energy storage.[1] Lithium metal batteries, such as the lithium-air (Li-air) battery and lithium-sulfur (Li-S) battery, are the promising next-generation energy storage systems because of their attractively high energy density (~3500 W h kg^{-1} in Li-air battery and ~2600 W h kg^{-1} in Li-S battery).[2] The Li metal anode possesses an unrivaled specific capacity (3860 mA h g^{-1}) and the lowest electrochemical potential (-3.04 V vs standard hydrogen electrode).[3] However, since rechargeable Li metal batteries emerged in the 1970s, the Li metal anode has long been considered "unsafe" because dendritic Li formed during electrodeposition could cause internal short circuit and safety hazards.[4] For practical applications of the Li metal batteries, efforts must be made to resolve the fundamental challenges of the Li metal anode.

The development of the Li metal anode is hindered by at least three issues. The first one is the formation and growth of Li dendrites during electrochemical deposition, which could penetrate through the separator and cause cell short circuit, imposing on the Li metal anode wide-ranging safety concerns. The dendritic Li could also lead to an electrical detachment of Li from the current collector and become "dead Li", significantly shortening the cycle life of the Li metal battery. The second problem lies in the interfacial instability of Li metal in the organic electrolyte. Due to the intrinsic high reactivity of Li metal in the organic electrolyte, corrosive reactions occur on the Li metal in most organic solvents. The side reactions on the Li metal surface will deplete the electrolyte, increase the resistance, and reduce the Coulombic efficiency and cell life. The third issue is the huge volume change of the electrode during Li deposition/dissolution, which is even more severe than that of the silicon anode

because Li deposition can lead to virtually infinite volume expansion. The volume effect further deteriorates the interfacial stability.

Recently, various approaches have been adopted to resolve these issues of the Li metal anode. The strategies for Li metal batteries with liquid electrolytes are schematically summarized in **Figure 1**. These strategies improve the Li metal anodes primarily by constructing rational Li host materials, protecting the Li interface via coating layers, optimizing the organic electrolytes, and modifying the separators. This review summarizes these methods and analyzes the protected Li metal anodes with organic electrolytes. While different approaches have been developed for Li metal batteries using organic electrolyte, Li metal is thermodynamically unstable in organic electrolytes.[5] In other words, these methods were effective to extend the lifetime of Li metal batteries but could not solve the intrinsic instability of Li metal in liquid-electrolyte batteries.

Solid-state electrolytes (SSEs) can fundamentally change the behavior of Li deposition and could be an ultimate solution to the issues of Li metal anode in liquid electrolytes. SSEs permit stable Li metal anodes since the solid nature of the electrolyte can effectively block Li dendrites and provide a large electrochemical stability window (0–5 V), superior thermal stability, and direct multiple cell stacking for high voltage design.[6] This non-liquid system allows batteries to tolerate both high voltages and temperatures, which enable solid-state Li metal batteries to be safer and possess higher energy densities than liquid electrolyte systems. Moreover, SSEs are single ion conductors and they have a high Li-ion transfer number close to 1 and negligible electronic conductivity. In Li-S batteries, the SSEs can eliminate the polysulfide dissolution problems. Therefore, it is expected to resolve the problems of Li metal anode in solid-state batteries. However, challenges remain on the interface between SSEs and electrodes due to thermodynamic instability in contact with Li metal anode, limiting the development of Li metal batteries.

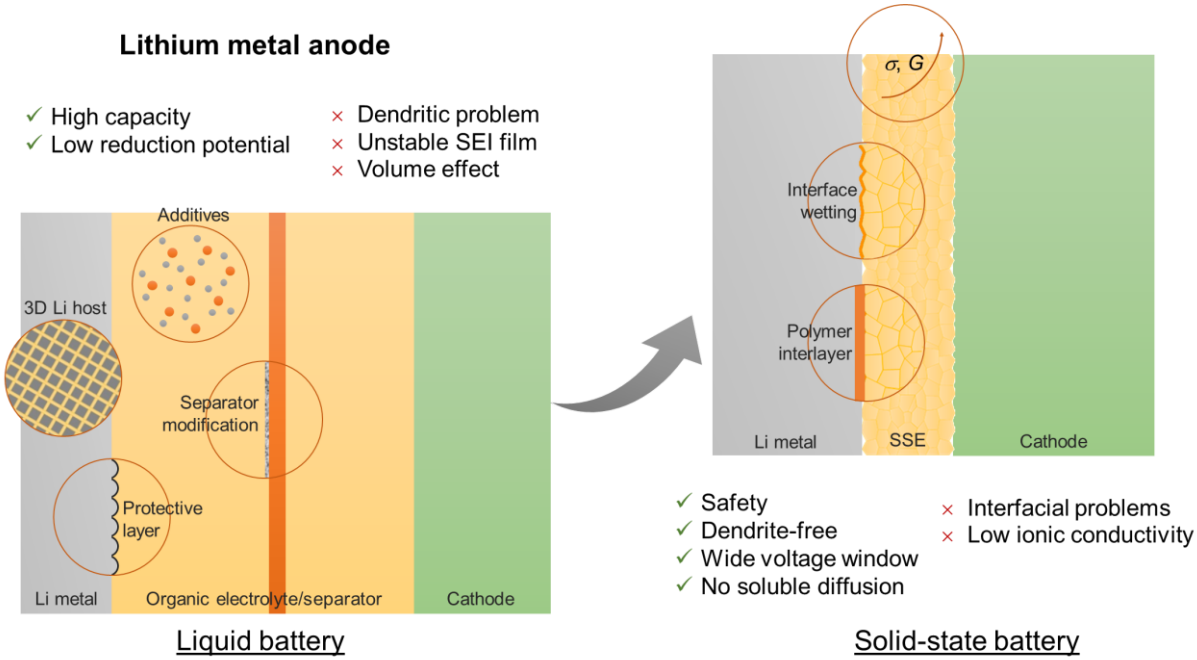

Figure 1. Development of Li metal anodes from liquid batteries to solid-state batteries. Advantages and existing problems of Li metal anodes and schematic of recent solutions for the Li metal anode with organic liquid electrolytes (left). Advantages, problems, and current strategies to address the problems of Li metal anode using SSEs (right).

This review further summarizes recent studies on Li metal anodes in conjunction with SSEs. Key challenges for solid-state Li metal batteries are the low Li-ion conductivity of SSEs and the interfacial resistance of Li metal and the solid electrolyte. Various approaches have been developed to improve the solid-state Li metal batteries by improving the ionic conductivity (σ) and modulus (G) of the SSEs, reinforcing the Li-SSE wettability, and utilizing polymer-inorganic hybrid configurations. This review discusses the research aiming to address the problems of Li metal anodes in solid batteries and provides an outlook for the future of Li metal batteries.

2. Li metal anodes in liquid-electrolyte batteries

Nonaqueous liquid electrolytes mainly consist of organic solvents and Li salts. Due to the high reactivity of Li metal, a solid electrolyte interphase (SEI) film is formed on the Li

interface in contact with the organic electrolyte. The SEI film is electronically insulative and ionically conductive, which is advantageous for Li batteries to prevent further corrosion to the Li metal. To obtain stable Li metal anode, it is critical to form a stable SEI film on the Li metal in the electrolyte.

The ideal SEI film on Li metal anode should be a thin yet hermetic layer with chemical and electrochemical stability, high Li-ion conductivity to transfer Li-ions, and robust mechanical strength to avoid Li metal penetration.[7] As illustrated in **Figure 2**, in ideal conditions (often at small current densities), Li deposition preserves the smooth surface and elevates the interfacial SEI while Li dissolution leads to SEI moving down. The SEI film remains intact during Li deposition/dissolution, passivating the Li interface constantly. However, the SEI film on Li metal has a complicated composition and is usually brittle.[8] At higher current densities, the inhomogeneous Li deposition and huge volume effect of Li metal anode would easily lead to the crack of the SEI film and growth of fresh dendritic Li; Li dissolution forms a pitted morphology, which also exposes fresh Li to the organic electrolyte.[9] As indicated in **Figure 2**, the SEI film repairs instantaneously at the dendrites or pits as a self-remedy process.[5] The repeated break/repair of SEI film will deplete the electrolyte, lower the Coulombic efficiency, and increase the cell impedance. The non-uniform SEI further causes the inhomogeneous deposition of Li metal, deteriorating the anode performance. Therefore, it is paramount for Li metal anode to form a stable, hermetic, and uniform SEI film on the Li metal for reversible Li deposition and dissolution.

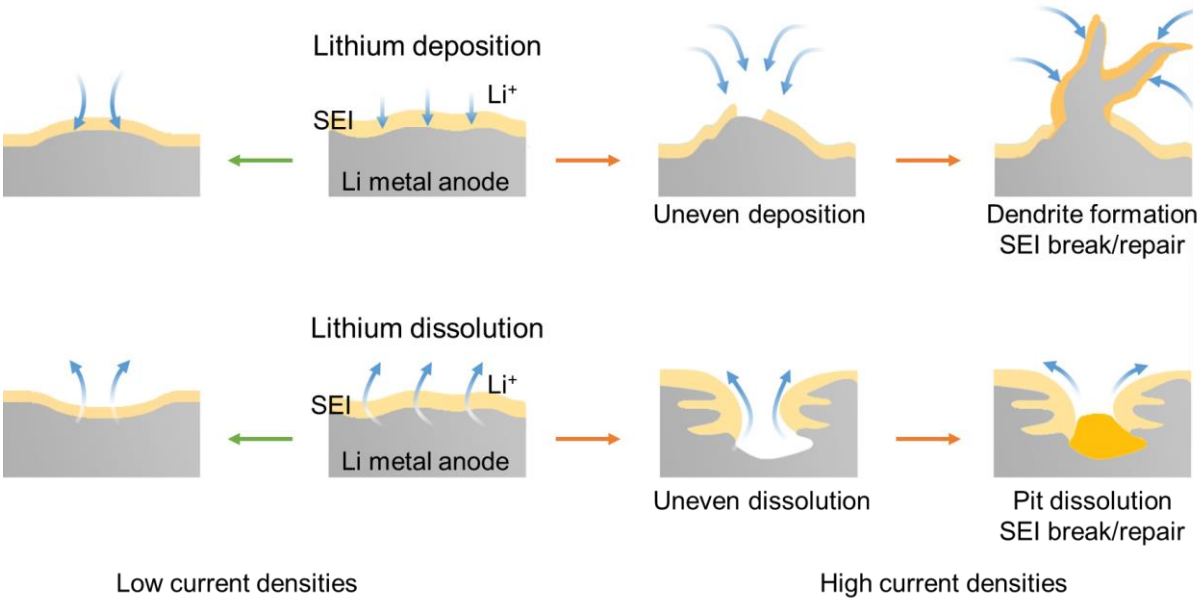

Figure 2. Schematic illustration of the evolution of the Li metal surface and SEI film during Li metal deposition and dissolution. At low current densities, Li is deposited/dissolved underneath the SEI layer and the SEI layer remains intact during Li deposition/dissolution. At higher current densities, volume changes (dendrite formation and surface pitting) lead to SEI break and repair. Modified with permission.[5] Copyright 2002, Elsevier.

2.1. Electrolyte modification

The composition of the SEI film on Li metal anode relies greatly on the electrolyte (solvent and salts) and additives (or impurities). Generally, the organic components in the SEI stem from the reactions between the Li metal and the solvent whereas the inorganic components come primarily from decomposition of the Li salts.[8] Rational choice of organic solvents, Li salts, and functional additives is desired to reinforce the SEI film on Li metal anode and improve its performance.[10]

2.1.1 Organic solvents

In conventional Li-ion batteries, carbonates, such as propylene carbonate (PC), propylene carbonate (EC), dimethyl carbonate (DMC), and diethyl carbonate (DEC), are widely applied as the solvents of the electrolytes. Considerable studies have been conducted to understand the SEI film in Li-ion batteries using carbonate-based electrolytes. The carbonate-based

electrolytes have also been employed in Li metal batteries.[11] However, despite their success in Li-ion batteries, the carbonate-based electrolytes show few merits in Li metal batteries in terms of Li dendrite suppression and cell life. Worse yet, studies have revealed that the carbonate-based electrolytes are not compatible with cathodes of Li-air and Li-S batteries, in which the carbonates decompose because of the nucleophilic attack by reduced oxygen species or polysulfides.[12]

Recently, electrolytes using ethers, such as 1,3-dioxolane (DOL), 1,2-dimethoxyethane (DME), and tetraethylene glycol dimethyl ether (TEGDME), as solvents have received more attention. The ether-based electrolytes have low viscosity and high ionic conductivity.[11] Moreover, unlike the carbonates, the ether-based electrolytes are compatible with high-energy Li metal batteries (Li-air and Li-S batteries). It is also found that the Li metal anode has a high Coulombic efficiency and low voltage hysteresis in the ether-based electrolytes.[3]

In addition to carbonates and ethers, some other organic solvents such as dimethylsulfoxide and acetonitrile have also been employed in Li metal batteries.[13] Recently, the room temperature ionic liquid (RTIL) has aroused tremendous interest in energy storage systems.[14] The RTIL has a low vapor pressure and is non-flammable. These features are favorable to the safety of Li metal batteries.[15] Studies on the compatibility of the RTIL and the Li metal have shown that some RTILs based on pyrrolidinium, imidazolium, and piperidinium can mitigate the Li dendrite formation and enhance the cycle stability of the Li metal anode.[16] The disadvantages of the RTIL-based electrolytes include the high viscosity and low ionic conductivity. Archer and co-workers studied RTIL and RTIL-SiO_2 nanoparticle hybrid electrolytes based on 1-methy-3-propylimidazolium (IM)[17] and 1-methy-3-propylpiperidinium (PP).[18] The hybrid electrolytes were synthesized by tethering IM-TFSI or PP-TFSI with SiO_2 nanoparticles and blending with 1 M LiTFSI in PC solution (illustrated in **Figure 3**a). The DC conductivity test shows that the PP-based electrolytes can reach a high conductivity approaching 1 mS cm^{-1} by tuning the volume fraction of SiO_2. The hybrid

electrolytes with a reasonable content of RTIL (IM or PP) also significantly increase the cell lifetime, which is characterized by the short-circuit time in Figure 3b. The RTIL-PC hybrid electrolytes, particularly the PP-based hybrid electrolytes, are efficient to increase the cell life and promote uniform Li deposition because of the benign conductivity, mechanical properties, and electrochemical stability.

Besides the RTIL-PC electrolytes, the RTIL-ether hybrid electrolytes have also been studied using *N*-propyl-*N*-methylpyrrolidinium TFSI ($Py_{13}TFSI$) and DOL/DME.[19] It is reported that by blending the $Py_{13}TFSI$ with DOL/DME and tuning the Li salt concentration, a stable SEI film is formed on the Li metal anode, which is schematically compared with Li metal anode in the conventional ether-based electrolyte in Figure 3c. The Li plating and stripping reversibility is remarkably improved. The optimized electrolyte using $Py_{13}TFSI$, DOL and DME hybrid solvent with 2 M LiTFSI shows an excellent cycling stability and a high Coulombic efficiency (99.1% after 360 cycles, Figure 3d). These studies clearly imply that developing novel electrolyte solvents is beneficial to mitigate the Li dendrite growth and anode interface problems.

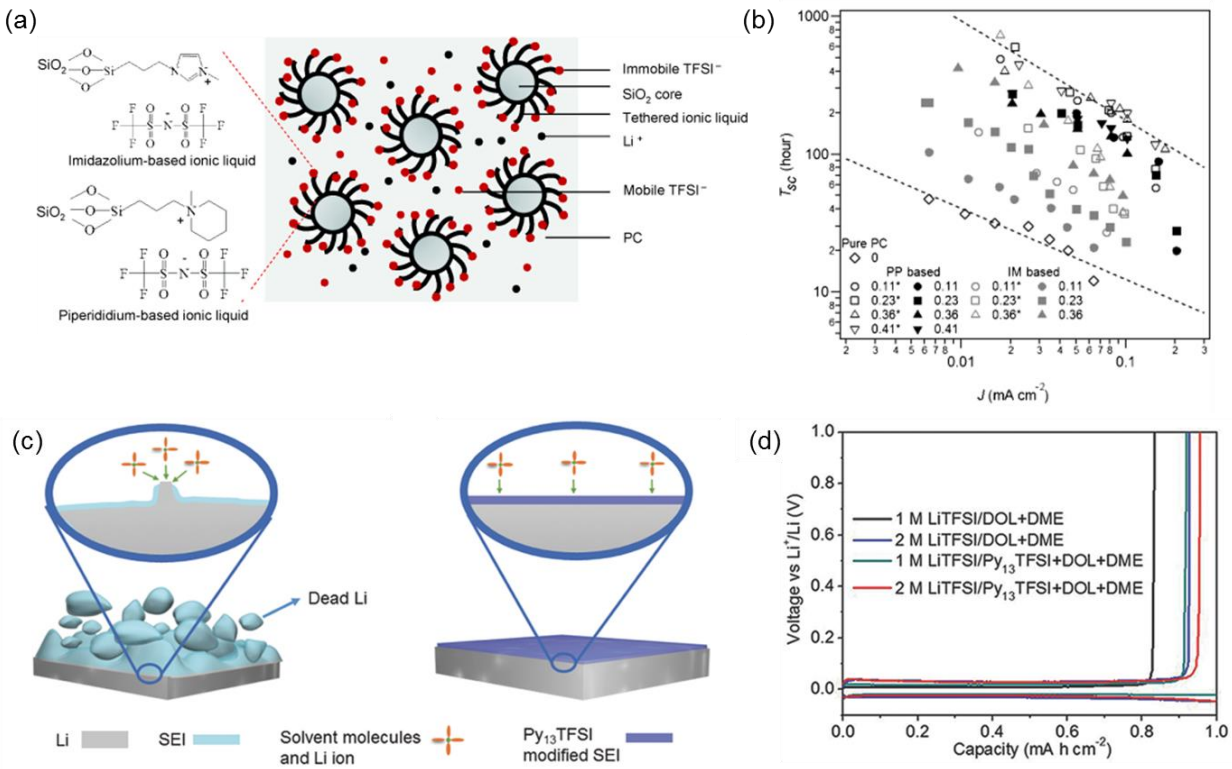

Figure 3. RTIL-based electrolytes for Li metal anodes. a) Scheme of the 1 M LiTFSI in SiO_2-RTIL-TFSI/PC hybrid electrolyte. b) Short-circuit time (T_{SC}) at different current densities (J) in Li symmetric cells using PP or IM based hybrid electrolytes with different volume fractions of SiO_2. a-b) Reproduced with permission.[18] Copyright 2014, Wiley. c) Schematic representation of Li metal deposition in different electrolyte systems. d) Discharge/charge voltage profiles of Li metal anodes in different electrolytes. c-d) Reproduced with permission.[19] Copyright 2016, Wiley.

2.1.2 Li salts

The other key component of the electrolyte is the Li salt. The Li salts used for Li metal batteries should not only meet essential requirements of the electrolyte (i.e., wide voltage window, high dissociation constant, high transfer number, etc.) but also be chemically and electrochemically compatible with the Li metal anode and the cathodes. The ideal Li salt should also facilitate the formation of thin and stable SEI films. The frequently used Li salts in Li metal batteries are $LiPF_6$, LiTFSI (bis(trifluoromethane)sulfonimide lithium salt), $LiSO_3CF_3$, $LiClO_4$, and so on. Aurbach *et al.* found that the $LiClO_4$ has lower reactivity with Li metal anode than other Li salts and are thus favorable for the Coulombic efficiency of Li metal anode.[20] However, the perchlorate with strong oxidability leads to safety concerns and is scarcely accepted in the battery industry.

$LiPF_6$ is a widely-used Li salt in Li-ion batteries and Li metal batteries though it is sensitive to moisture. LiTFSI, $LiSO_3CF_3$, and $LiN(SO_2F)_2$ (LiFSI) are another type of promising salts, which have a high dissociation constant, high-voltage stability, and good thermal and moisture stability. These salts are extensively used in Li metal batteries; however, they show little effect on the interface stability and the dendritic Li morphology. As an alternative to single Li salt, electrolytes using binary salts such as LiTFSI-LiFSI have been developed to

balance the ionic conductivity and viscosity of the electrolyte for homogeneous Li deposition in Li-S batteries.[21]

The concentration of the salt in the electrolyte has a significant effect on the ionic conductivity, Li-ion transfer, and viscosity of electrolyte. Generally, the Li deposition behavior can be improved by increasing the salt concentration. Compared with the standard 1 M molarity, a concentrated electrolyte provides sufficient Li-ion resources and high viscosity for suppressing the formation and proliferation of Li dendrites. When the concentration of $LiAsF_6$ in PC is increased from 0.5 M to 1.5 M, corresponding Coulombic efficiency is improved from 72% to 85%.[22] Zhang *et al.* dissolved 4 M LiFSI in DME, in which the Li metal anode can cycle at 4 mA cm^{-2} for 1000 cycles with a Coulombic efficiency of ~98.4%.[23] An ultrahigh concentration electrolyte, or so-called 'Solvent-in-Salt' electrolyte, employing 7 M of LiTFSI in the electrolyte, has been reported to reinforce uniform Li deposition.[24]

2.1.3 Functional additives

Various functional additives at small concentrations in the electrolyte have been considered beneficial to the battery performance in prior studies and have been utilized widely in Li-ion batteries. In Li metal batteries, electrolyte additives have also been adopted to improve the Li-electrolyte interface, modify the properties of the SEI film on Li metal anode, and minimize the side reactions at the Li interface. Various electrolyte additives that have been previously used in Li-ion batteries are employed in Li metal batteries, for which functions and mechanisms of each are briefly summarized in Table 1. Generally, these conventional additives have proven advantageous to stabilize the interface, improve the Coulombic efficiency, and reduce the interface impedance, but are not effective enough to eliminate the growth of Li dendrites.[3, 7]

Table 1. Electrolyte additives and their functions in Li metal batteries.[3, 7]

Additives	Function	Mechanism
CO_2 [8a]	Stabilize the interface	Forming Li_2CO_3 protective layer
HF [25]	Stabilize the Li deposition and improve the Coulombic efficiency	Forming LiF-Li_2O layer
Vinylene carbonate[26]	Stabilize the interface	Ring-opening polymerization at Li surface to form a film
Fluoroethylene carbonate (FEC)[27]	Improve the Coulombic efficiency and suppress the dendrite formation	Producing a LiF-rich surface film with uniform structure
2-Methylfuran[28]	Improve the Coulombic efficiency and reduce the impedance	Ring-opening polymerization at Li surface to form a film
Metal ions (e.g., Na^+, Mg^{2+})[29]	Suppress the dendrite formation and improve the Coulombic efficiency	Forming superficial thin layers of alloys with Li
Inert additives (e.g., toluene)[30]	Reduce the cell impedance	Accumulation at interface to form a film

Novel functional additives have been developed for Li metal batteries. One of the most commonly used additives for the Li-S battery is $LiNO_3$. The $LiNO_3$ additive can passivate the Li metal anode to inhibit the reaction between Li metal and polysulfides and thus eliminate the "shuttle effect" (dissolved lithium polysulfides shuttle and redox repeatedly between the S cathode and Li metal anode).[31] Recently, extensive studies have been reported using $LiNO_3$ for Li anode passivation.[32] Because of the strong oxidation of $LiNO_3$, the additive creates a surface film composed of LiN_xO_y in addition to the native film (Li_2CO_3, LiOH, Li_2O, etc.). The LiN_xO_y film could keep growing during cycling and cause increased resistance. When the $LiNO_3$ additive cooperates with Li_2S_n (n = 4–8) additives, or dissolved Li_2S_n in Li-S batteries, a synergetic effect is found as reduced products of $LiNO_3$ and Li_2S_n co-precipitate and further convert to a smooth and stable SEI film on the Li surface (**Figure 4**). By tuning the concentrations of the $LiNO_3$ and Li_2S_n, the Li metal anode can benefit most from the synergetic passivation effect of the additives. Using an ether-based electrolyte, 1 M LiTFSI in

DOL/DME, with the addition of 0.18 M Li_2S_8 and 5 wt.% $LiNO_3$, the Li metal anode is free from dendrite problems with a capacity up to 6 mA h cm^{-3} at a current density of 2 mA cm^{-2}. The Li metal anode also exhibits excellent cycle stability with a high Coulombic efficiency (> 99%) for 300 cycles at 2 mA cm^{-2}.[32b] These appealing results demonstrate the beneficial synergetic effect of the $LiNO_3$ and Li_2S_n additives for Li metal batteries. A ternary-salt (LiTFSI–$LiNO_3$–Li_2S_5) electrolyte has been proposed based on the synergetic effect for dendrite-free Li metal anode.[33]

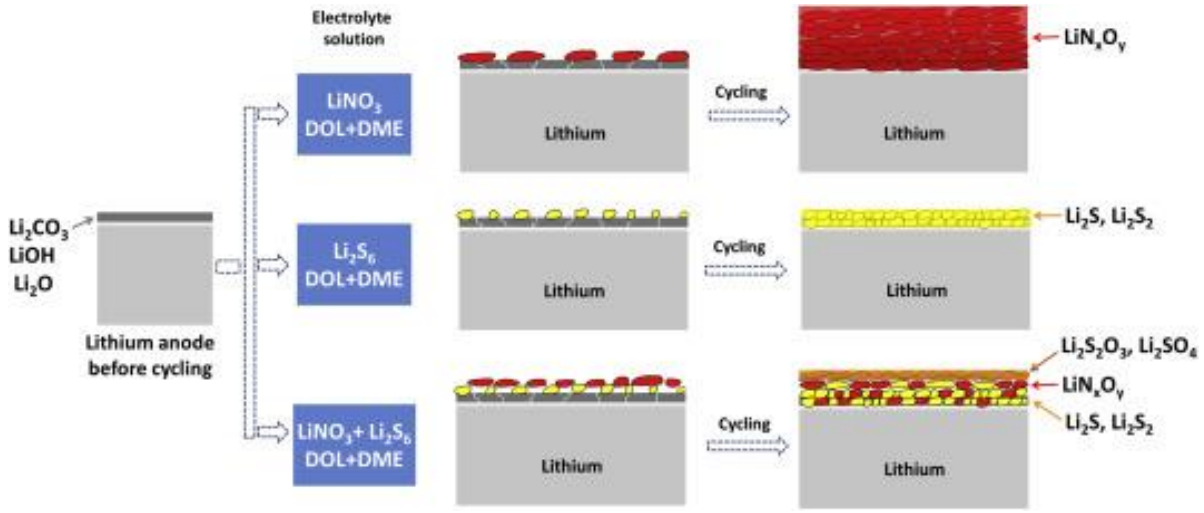

Figure 4. Scheme of the SEI film formation and evolution on Li metal anodes in ether-based electrolytes with different additives. Reproduced with permission.[32a] Copyright 2014, Elsevier.

Based on a self-healing electrostatic shield mechanism, Zhang and co-workers proposed to use Cs^+ or Rb^+ cations with low concentrations, which have lower reduction potentials than Li^+ in the electrolytes, to form an electrostatic shield at Li metal surface for smooth Li deposition.[34] As illustrated in **Figure 5**a, once a Li dendrite root is formed during Li deposition, the non-Li cations (Cs^+ or Rb^+) will be accumulated surrounding the Li tip but will not be reduced (because of their low reduction potentials). The non-Li cations adsorbed on the tip spontaneously form a positively charged electrostatic field and repel more incoming Li ions. Consequently, further Li deposition on the dendrite root, which could have formed Li

dendrites, is prevented and Li ions are forced depositing adjacently. Therefore, as illustrated in Figure 5b and demonstrated by the scanning electron microscope (SEM) image in Figure 5c, a smooth Li deposition is obtained without the pernicious dendritic morphology. The non-Li ions are not consumed during cycling; thus, the self-healing electrostatic shield mechanism is consistently effective for a long-term cycle. Based on this mechanism, the Li|$Li_4Ti_5O_{12}$ cell using the PC-based electrolyte with 0.05 M Cs^+ additive exhibits excellent cycling stability and high Coulombic efficiency of 99.86% (Figure 5d). The additives in the electrolyte effectively suppress dendrite growth on the Li anode, though the Coulombic efficiency of Li deposition in the electrolyte with the Cs^+ additive is yet to be improved. A further study shows that with the Cs^+ additive in the electrolyte, the growth of dendrite-free Li metal forms aligned and compact nanorods.[35] The smooth deposition of Li metal is a synergistic result of the Cs^+ additive and the SEI layer.

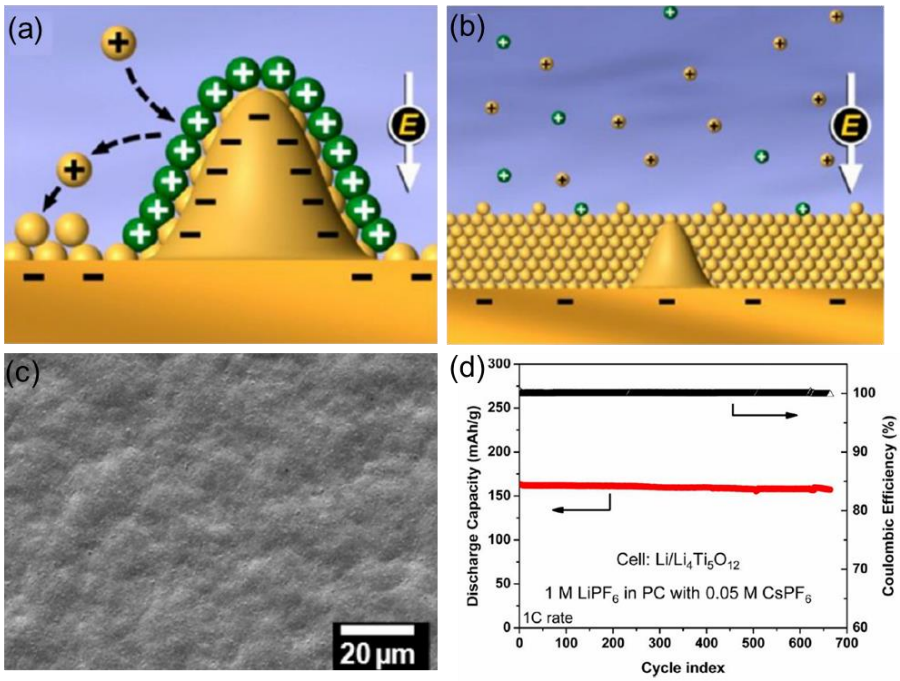

Figure 5. Illustration of the Li deposition process with Cs^+ or Rb^+ cation additives based on a self-healing electrostatic shield mechanism: a) Cs^+ or Rb^+ cations accumulated near the Li tip, forming a positive charge shield that repels ensuing deposition of Li ions; b) a smooth deposition is expected with Cs^+ or Rb^+ additives based on this mechanism. c) SEM image of

the morphology of Li deposition in 1 M $LiPF_6$/PC with 0.05 M $CsPF_6$ additive. d) Cycling performance and Coulombic efficiency of Li|$Li_4Ti_5O_{12}$ cell using the electrolyte of 1 M $LiPF_6$/PC with 0.05 M $CsPF_6$ additive. Reproduced with permission.[34] Copyright, 2013, American Chemical Society.

Various other additives have been studied for different purposes in Li metal batteries.[36] Archer and co-workers reported Li haloid salts as additives in conventional PC electrolytes.[37] The halogenated salt additives can reinforce uniform Li deposition by forming a conformal crystalline SEI film on the Li metal anode. When 30 mol% LiF is employed in the Li metal battery, smooth Li deposition is obtained without signs of electrodeposition instability or dendrite formation. Li symmetric cells using the electrolyte with the LiF additive shows markedly increased cycle life. Using 30 mol% LiF additive, more than a 30-fold cell lifetime enhancement can be achieved, demonstrating the effectiveness of LiF to extend the cell lifetime. A trace amount of H_2O has also been reported as an additive to create a thin and dense LiF-rich SEI film, which renders Li deposition uniform and dendrite-free.[38]

The use of small amounts of electrolyte additives generally does not affect the primary properties of the electrolytes (such as ionic conductivity) but is often critical in affecting electrolyte performance. The additives can significantly improve the Li-electrolyte interface stability and Li cycling efficiency. Novel additives can be applied in Li metal batteries for different functions beyond the electrochemical performance. For example, flame retardants such as phosphites have been adopted as additives to inhibit the flammability of organic electrolytes for safer Li metal batteries.[39]

2.2 Surface protecting layer (artificial SEI film)

The SEI film generated on Li anode in organic electrolyte serves as a protecting layer for Li metal anode that can prevent side reactions between the Li metal and organic electrolyte. An ideal protective layer should be chemically and electrochemically stable, mechanically robust

to inhibit Li dendrite penetration, and flexible to accommodate the volume changes during Li plating/stripping. The SEI film formed in the electrolyte in batteries (or *in-situ* formed SEI) cannot fully meet these criteria because it is prone to cracking by Li dendrites. In this context, constructing an additional stable and robust film as a protective layer (or so-called "artificial SEI film") is worthwhile to reinforce the protection effect on the Li metal anode. A facile method to form the artificial SEI film is to generate a passivation layer on the Li metal surface by chemical pretreatments prior to electrochemical reactions.

The SEI film on the Li metal can be corroded by the electrolyte because of the partial dissolution of the native SEI film (composed of Li_2CO_3, LiOH, and Li_2O). To enhance the stability of the SEI film, Guo and co-workers proposed to generate an artificial Li_3PO_4 layer on the Li metal (**Figure 6**a) by pretreating Li metal in polyphosphoric acid (PPA).[40] Through controlling the pretreating conditions, a uniform Li_3PO_4 SEI layer with an effective thickness of ~50 nm was generated on the Li metal replacing the pristine native film (Li_2CO_3 etc.). The Li_3PO_4 layer is chemically stable in the organic electrolyte, significantly reducing breakage of the SEI film and corrosion of the Li metal. As measured by the atomic force microscopy (AFM) in Figure 6b, the Li_3PO_4 layer possesses a high Young's modulus (10–11 GPa), effectively suppressing the growth of dendritic Li (a film with a modulus greater than 6 GPa is predicted sufficient for this purpose.[41]). Owing to the high ionic conductivity and high modulus of the Li_3PO_4 thin film, the PPA-pretreated Li metal anode exhibits a smooth and even surface after Li plating/stripping, free from the dendritic problem (Figure 6c). The Li metal anode with Li_3PO_4 SEI film shows extended cycling life. Using the PPA pretreated Li metal anode and the $LiFePO_4$ cathode, the full cell shows better cycling stability and smaller voltage polarizations than that using the untreated Li metal anode. Magnetron sputtering has also been employed to deposit a conformal Li_3PO_4 thin film on Li metal, which has reduced grain boundary, controllable thickness, and isotropic amorphous nature.[42] The nanoscale

amorphous protective films render Li deposition homogeneous and improve the anode lifespan.

Similar chemical pretreating approaches were conducted in RTIL,[43] tetraethoxysilane,[44] and so on to form durable artificial SEI films. A layer of Li-ion conductor Li_3N was formed on Li metal as a protective film by in-situ reaction between Li metal and N_2 gas.[45] The tight and dense Li_3N film improves the Li cycling efficiency, homogenous Li deposition, and the electrochemical performance of the Li-S battery. A more complicated chemical pretreating approach has been reported. Li foil was exposed to tetrahydrofuran, O_2 atmosphere, and trimethylsilyl chloride in sequence to produce a thin and dense protective film.[46] In addition to chemical reactions, Li surface can be pretreated electrochemically to form protective SEI film.[47] For example, the Li metal anode can form an artificial protective film by electrochemically pretreating in a symmetric cell with a TEGDME-FEC electrolyte before reassembled in Li-air batteries.[47a]

Superior to the simple pretreatment in solutions (or gas atmosphere), an advanced surface modification method, atomic layer deposition (ALD), has been utilized for Li surface passivation. The ALD technique can create atomically precise control and form conformal coating films. Moreover, ALD is usually conducted in an inert environment at relatively low temperatures (lower than the melting point of Li), allowing surface coating on Li metal by the ALD method. ALD coating is believed an ideal surface pretreating method suited to Li metal passivation.[48] As illustrated in Figure 6d, Al_2O_3 can be directly deposited on Li metal foil via ALD and form stable and ion-conductive $LiAlO_x$ solid electrolyte after lithiation. The Al_2O_3 coating layer via ALD on Li metal shows improved stability against the corrosion by moisture, CO_2, and organic solvents. The Li protection effect is found proportional to the thickness of the ALD coating layer (Figure 6e).[48a] In Li-S batteries, the Li metal with the Al_2O_3 layer exhibits improved stability in the corrosive sulfur-rich electrolyte (containing dissolved sulfur and polysulfides). The Li metal anode with 14 nm Al_2O_3 is found to reduce the self-discharge

effect and initial capacity loss significantly in the Li-S battery compared with the bare Li metal anode. The ALD-Al_2O_3 protection layer also improves the capacity retention of the Li-S battery due to the reduced Li metal corrosion (Figure 6f). Even an ultrathin (~2 nm) ALD-Al_2O_3 layer can suppress the Li metal dendrite growth during the initial cycles,[48b] indicating the favorable protection for Li metal anode via the ALD surface engineering. Besides Al_2O_3, an ultrathin and ion-conducting Li_xAl_yS film coated via ALD has been found effective for stabilizing the Li-electrolyte interface and suppressing Li dendrite growth.[48c]

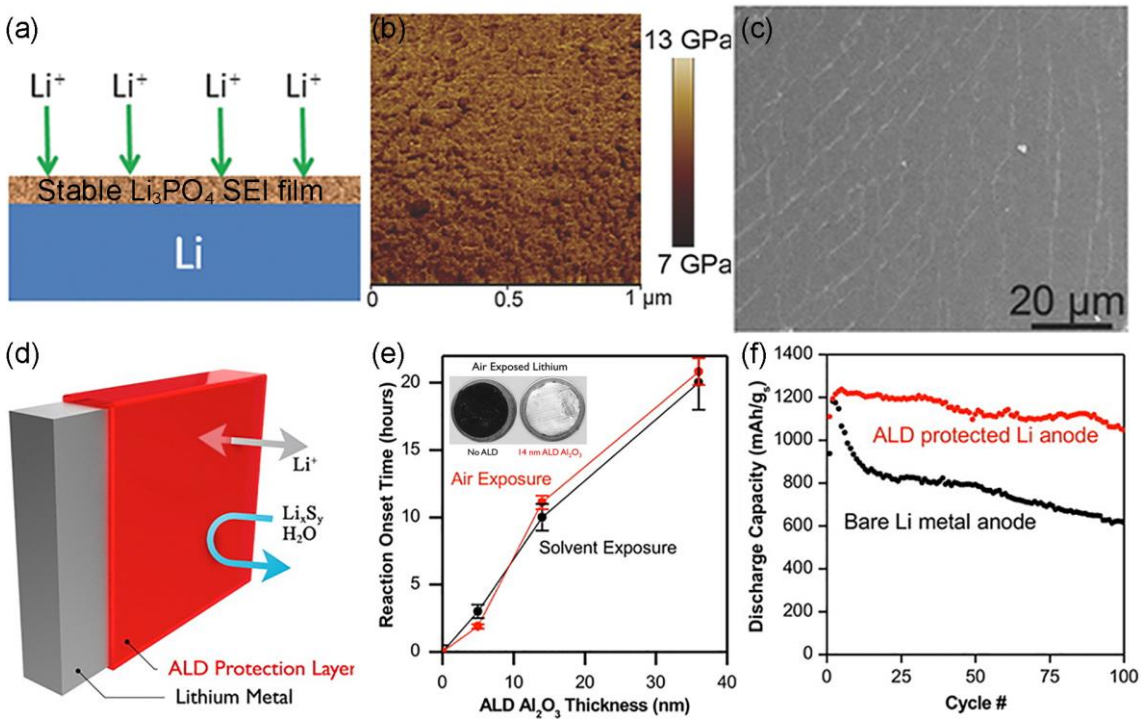

Figure 6. Artificial SEI films for Li protection. a) Schematic illustration of Li deposition on Li metal surface covered by stable Li_3PO_4 SEI film. b) Young's modulus mapping image of the PPA-pretreated Li metal showing the high modulus of the surface layer. c) SEM image of the PPA-pretreated Li metal anode after cycling in a Li|$LiFePO_4$ battery. a-c) Reproduced with permission.[40] Copyright 2016, Wiley. d) Schematic diagram showing Li metal anode protection via ALD deposited Al_2O_3. e) Reaction onset time of Li metal exposed to air and the organic solvent (PC) with different ALD-Al_2O_3 thicknesses. f) Discharge capacities of Li-S batteries with bare Li metal anode and ALD protected Li anode (14 nm Al_2O_3 coating layer). d-f) Reproduced with permission.[48a] Copyright 2015, American Chemical Society.

The protective layers (or artificial SEI films) formed via chemical/electrochemical pretreatment, ALD, and magnetron sputtering are generally thin films formed on the Li metal. The preformed artificial SEI films have acceptable ionic conductivity for Li migration. However, these films are often thin, brittle, and vulnerable to crack due to the volume effect of the Li anode during extended cycling. Different from the chemical or electrochemical pretreating method, physical covering/coating interlayers on the Li metal anodes have been reported as an ex-situ coating strategy for Li metal protection. The physically coated interlayers generally possess an advantageous mechanical strength for suppressing Li dendrites. Moreover, these interlayers offer more opportunities for material and structure design, which would greatly advance the development of Li metal anodes.

Various physically coating interlayers have been proposed for Li metal anodes. An innovative example of the ex-situ protective layer is a monolayer consisting of interconnected hollow carbon nanospheres designed by Zheng *et al.*[37] As illustrated in **Figure 7**a, the monolayer is loosely attached to the current collector surface and moves up and down together with the SEI film during Li plating and stripping. The hollow carbon nanosphere monolayer has an extremely high Young's modulus (~200 GPa) to suppress Li dendrite growth and mechanical flexibility to accommodate the volume change during Li plating. With the monolayer coating, Li metal is deposited beneath the hollow carbon nanospheres, elevating the nanosphere monolayer, forming columnar rather than dendritic Li (Figure 7b). Electrochemical cycling at 0.25, 0.5, or 1 mA h cm^{-2} of the nanosphere-coated Li anode shows high Coulombic efficiency (~99%) for over 150 cycles, demonstrating the interfacial engineering on Li metal anode a promising strategy. The interfacial protection effect was also achieved by hexagonal boron nitride and graphene.[49] The boron nitride and graphene thin films have a high mechanical strength to suppress Li dendrites and excellent chemical stability to passivate the Li-electrolyte interface.

A potential drawback of the electronically conductive layer (the carbon nanosphere monolayer has an electronic conductivity of ~7.5 S cm^{-1} [37]) is that it could lead to electron delivery across the interlayer, Li deposition on top of the interlayer, and finally failure of the protection effect. Robust and flexible polymer films that are electronically insulating are hence promising as protective coating layers for Li metal anodes. Polymer coating layers with high viscoelastic and self-healing properties are extremely desired for dendrite suppression.[50] Zhu *et al.* proposed a modified poly(dimethylsiloxane) (PDMS) thin film with nanopores serving as a protective layer for improving Li metal anode (Figure 7c). Since PDMS does not conduct electrons or Li-ions, nanopores in the PDMS film are created by hydrofluoric acid etching to promote Li-ion transport. Thus, the PDMS film can enable uniform Li deposition and suppress Li dendrite formation by the high modulus and flexibility. The Li metal anode modified by the PDMS film exhibits smooth and flat surface after 1 mA h cm^{-2} Li deposition (Figure 7d). The modified Li metal anode has a Coulombic efficiency of ~95% for 200 cycles. The nanoporous non-conductive polymer protecting layer provides a complementary method to develop dendrite-free Li metal anodes.

A polyimide film with aligned nano- and micro-sized channels has been reported to coat on the Li metal for a stable Li deposition.[51] Homogenous Li^+ flux through the aligned nanochannels of the polyimide film leads to a uniform Li nucleation and thus improved cycle life and Coulombic efficiency (97.6% for 240 cycles at 1 mA cm^{-2}). Electronically insulating 3D oxidized polyacrylonitrile nanofibers on Cu current collector was fabricated by electrospinning to guide uniform Li deposition.[52] Li metal is deposited in the 3D polymer layer and shows stable cycling performance with a Coulombic efficiency of ~97% at 3 mA cm^{-2} over 120 cycles.

In addition to the polymer membranes, inorganic interlayers with nanopores are developed as protecting layers for Li metal anodes. Recently, a 3D glass fiber cloth is reported as modification layer between the electrode and the separator to stabilize the Li metal anode. The

non-conductive glass fiber framework allows epitaxial Li growth only from the electron conductor (former Li metal).[53] The glass fiber matrix assists in homogenizing Li-ion flux. Li metal is deposited uniformly underneath glass fiber layer and grows epitaxially within the matrix without forming any dendrites. The dendrite-free Li deposition stabilizes the SEI film of the Li metal anode and improves the Coulombic efficiency of the anode from 80% to 97% at a current density of 1.0 mA cm^{-2}. These nanoporous layers serve as surface protection layers for uniform Li-ion flux as well as Li metal hosts to inhibit the growth of Li dendrites. It is believed that ceramic membranes (such as the anodic aluminum oxide membrane) with pores smaller than the diameter of mossy Li whiskers can lead to a transition of the Li formation mechanism and block the mossy Li.[54]

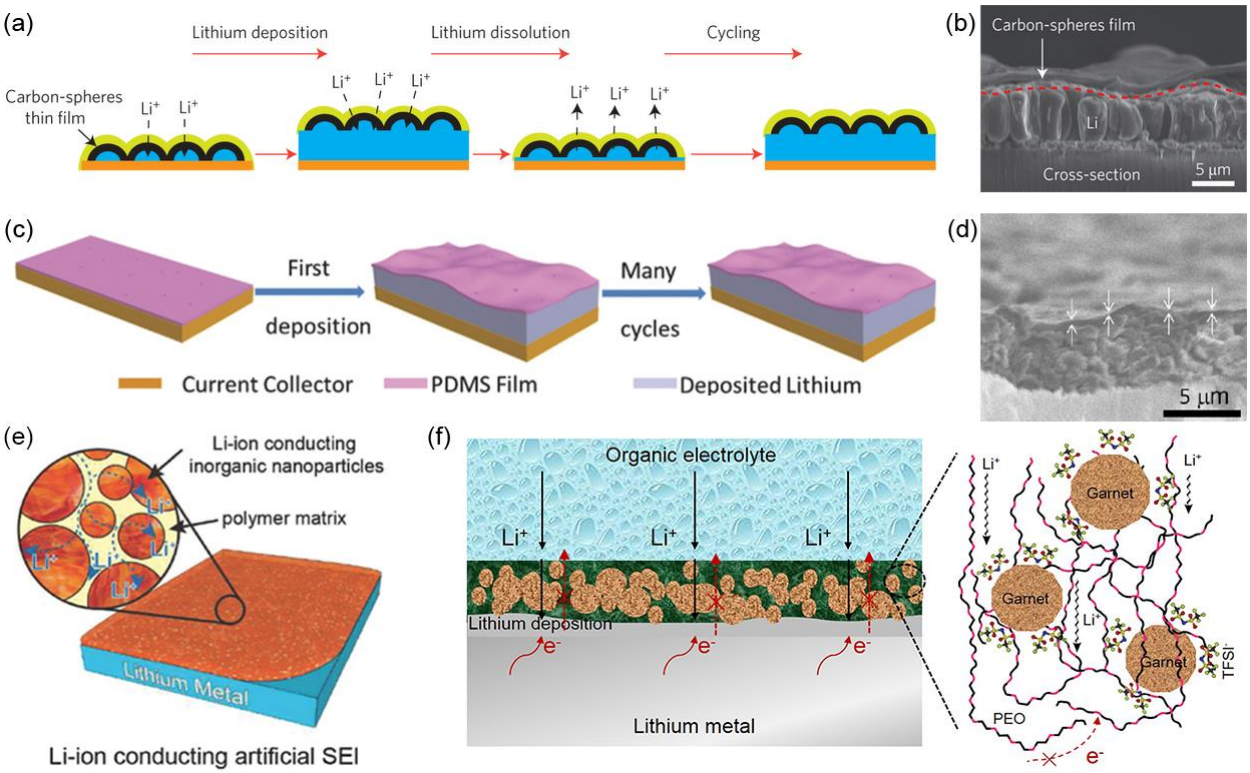

Figure 7. Ex-situ protective interlayers for Li metal anodes. a) Schematics of Li deposition and dissolution on a Cu substrate modified by a hollow carbon nanosphere layer. b) Cross-sectional SEM image showing the Li deposition elevating the hollow carbon nanosphere layer. a-b) Reproduced with permission.[37] Copyright 2014, Wiley. c) Schematic representation of Li deposition on the current collector coated with the PDMS thin film, which suppresses the

dendrite formation and enables uniform deposition for many cycles. d) Cross-sectional SEM image of initial Li deposition on PDMS (indicated by the arrows) coated Cu foil. c-d) Reproduced with permission.[55] Copyright 2016, Wiley. e) Schematic illustration of Li metal protected by Li-ion conducting artificial SEI composed of Cu_3N and styrene butadiene rubber. Reproduced with permission.[56] Copyright 2016, Wiley. f) Schematic of Li deposition with the protection of garnet and PEO hybrid ion-conducting film. Reproduced with permission.[57] Copyright 2017, Springer.

An intrinsic advantage of the non-conductive protecting layers (polymer films or inorganic oxides) is that they enable Li metal epitaxial growth only from the electron-conducting substrates and Li metal is deposited underneath the interlayer or embedded in the interlayer. An ion-conducting and electron-insulating layer is better than non-conducting layers in this scenario because it can facilitate Li-ion transfer. Li-ion conductors have been utilized as coating layers to protect Li metal anodes. The LISICON (Lithium Super Ionic Conductor) film was applied as Li-ion conductor and separator for aqueous Li metal batteries (mostly aqueous Li-air battery).[58] The LISICON film was also studied as coating layer combined with a sandwiched polymer membrane saturated with Li salt.[59] The ceramic Li-ion conductor is utilized to isolate Li from aqueous electrolyte for a stable and safe aqueous Li metal battery. However, it remains unclear how the ceramic Li-ion conductor affects the Li deposition behavior and the Li interface stability, and how the stiff ceramic would accommodate the Li volume expansion during Li plating.

A superior approach is to fabricate a polymer-ceramic hybrid ion conductive layer on the Li metal as an artificial SEI layer. The hybrid ion-conducting layer is expected to have favorable ionic conductivity for Li-ion migration and desired flexibility to accommodate Li volume change. As schematically depicted in Figure 7e and 7f, ion-conducting polymers are used as the framework of the coating layers and ceramic nanoparticles (Cu_3N or garnet-type Li-ion

conductor) are dispersed in the polymers,[56-57] greatly enhancing the mechanical strength of the coating layer. The inorganic nanofillers either are Li-ion conductors (garnet-type Li-ion conductor in Figure 7f, see below for more discussion about garnet) or are converted to Li-ion conductors (Cu_3N converted to Li_3N in Figure 7e). Thus, the high ionic conductivity of the coating layer is ensured for Li-ion transfer and deposition. The electronically insulative layers block electron passage and constrain the Li deposition between the interlayer and the current collector. More studies should be done to determine the optimal modification interlayers for Li metal anode, which should provide homogeneous Li-ion flux for a uniform Li deposition, mechanical strength to suppress the dendrite growth, flexibility to accommodate the volume change, and chemical stability for Li-electrolyte interface stability.

2.3 Electrode framework design

The inhomogeneous Li-ion flux distribution usually leads to the non-uniform Li nucleation. The non-uniform Li nucleation on the planar electrodes further induces the inhomogeneous Li deposition and dendrite proliferation. Recently, nanotechnology has greatly benefited the development of Li metal anodes. Rational 3D electrode frameworks with novel architectures have been designed to control the Li plating/stripping behavior and improve the Li metal anode stability.[52] The ideal framework for Li metal anode should hold a large specific surface area to reduce the local current density and create a homogeneous Li-ion flux, which are crucial for uniform Li-ion nucleation. Porous structure with sufficient pore volume in the Li substrate is desired to accommodate the Li volume change effectively upon cycling. In addition, the Li host substrate should possess mechanical and electrochemical stability, high electrical or ionic conductivity for fast electron/ion transfer, and a low gravimetric density for a high energy density.

Among the various substrate materials, the widely adopted 3D current collectors are carbon-based materials or metallic frameworks.[52] These electrically conductive substrates with 3D

nanostructures can offer a network of free electron pathways and provide sufficient contact with Li-ion flux in liquid electrolytes, enabling fast charge transfer and uniform Li nucleation. The nanostructured Li metal anodes are realized using the 3D nanostructures with electrochemically deposited Li or 3D host materials with pre-loaded Li.

Among the carbon-based host materials, a spatially heterogeneous 3D current collector was reported by Ji and co-workers using modified carbon papers, which prevents Li deposition towards the separator. As shown in **Figure 8**a, a thin layer of insulating SiO_2 or SiC coating was applied onto the line-of-sight side (facing toward the separator) of the pristine carbon paper. The spatially heterogeneous insulating property from SiO_2 or SiC coating forces the Li ions to deposit on the backside of the carbon paper, resulting in a surface dendrite-free Li deposition and an inhibition of short-circuiting even at 4 mA cm^{-2} after a deep Li deposition of 28.8 C cm^{-2}.[60]

Recently, Zhang's group proposed an unstacked graphene framework with nano-sized hexagonal drums for Li deposition. As shown in Figure 8b, the novel anode forms a sandwich structure with SEI layer on the top, deposited Li metal in the center and graphene framework at the bottom. The nano-sized drums provide a large specific surface area (1666 m^2 g^{-1}) and pore volume (1.65 cm^3 g^{-1}), which renders an ultralow local current density and enables a homogeneous Li deposition beneath the SEI. Compared with planar Cu, the graphene-based anode demonstrates an improved cycling stability for 800 cycles with a small hysteresis of 150 mV at 2 mA cm^{-2} and a capacity of 0.5 mA h cm^{-2} (Figure 8c), indicating an effective inhibition of Li dendrites by the decreased local current density.[61] In addition, nanostructured graphite electrodes within deposited Li metal can achieve the improved cycling stability by effectively accommodating Li volume change in the 3D structures and suppressing the growth of Li dendrites.[62]

Cui's group proposed a unique nanocapsule structure to improve the stability for Li metal anodes, which contains Au nanoparticles as Li nucleation seeds inside the hollow carbon

spheres. The Li deposition observation with in situ transmission electron microscopy reveals that the deposited Li metal predominantly occurs on the Au seeds inside the hollow carbon spheres. This selective deposition and Li encapsulation inside the hollow carbon sphere eliminate the growth of Li dendrites and improve the cycling stability with a Coulombic efficiency of ~98% over 300 cycles.[63]

Compared with conventional planar current collectors, the carbon nanotubes sponge possesses a large specific surface area (300–400 $m^2 \cdot g^{-1}$) with a high porosity (>99%), which can afford as an ideal 3D host for Li metal anodes.[64] Hence, Zhang *et al.* [65] developed a 3D current collector as a Li deposition host by growing a conformal layer of Al_2O_3 on the carbon nanotubes sponge via ALD. The Al_2O_3 layer with good chemical stability and high mechanical strength affords a robust protection to enhance the interface between 3D electrode and electrolyte. The modified electrodes present stable cycling with an improved Coulombic efficiency in carbonate electrolyte without additives.[65]

In addition to using the porous carbons as Li host material, porous metal or alloy substrates have also been developed for hosting Li anode. A fibrous Li_7B_6 alloy framework was reported for suppressing the Li dendrites.[66] Due to the decreased local current density in the nanostructured anode, the Li_7B_6 anode with embedded Li metal exhibited enhanced cycling stability in high-energy-density Li-S batteries.

Commercial Cu foil is one of the most common metallic current collectors used in Li-ion batteries. Nevertheless, the initial plating of Li metal on planner Cu leads to inhomogeneous Li nucleation, followed by severe Li dendritic growth and Coulombic efficiency drop afterward (Figure 8d). To solve this problem, Guo's group fabricated a novel 3D Cu with submicron pores (median pore diameter: 2.1 μm) to host Li metal as well as a high areal pore area for homogeneous Li deposition.[67] Compared with planar Cu foils, the 3D Cu exhibits excellent cycling stability for 600 h without short circuit signals (Figure 8e).[67] Yang and co-workers developed a facile method to produce a 3D porous Cu by dealloying Zn from Cu-Zn

alloy. The porous Cu exhibits a pore size distribution from 200 nm to 2 μm and furthermore, many protuberances on the inner surface can provide charge centers and nucleation sites for Li metal deposition.[68] A free-standing Cu nanowires membrane was also synthesized simply by self-evaporation of the suspension of Cu nanowires. The Cu nanowires can hold 7.5 mA h cm^{-2} of Li metal totally inside the pores with the area of 1.1 cm^2 without Li dendrites.[69] The above-mentioned 3D Cu electrodes were demonstrated to deliver a high Coulombic efficiency (>97% after 200 cycles) owing to the inhibition of Li dendritic growth.[67-70] Furthermore, the full cells integrated with Li anodes with 3D Cu current collectors show an improved cycling stability and higher rate capability, in comparison with the cells using Li anodes with planar Cu.[68-69] The porous structure of 3D Cu with a high electroactive surface can dramatically decrease the local current density and effectively accommodated Li metal in the pores, which should account for the significant suppression of Li dendrites during the repeated cycles.

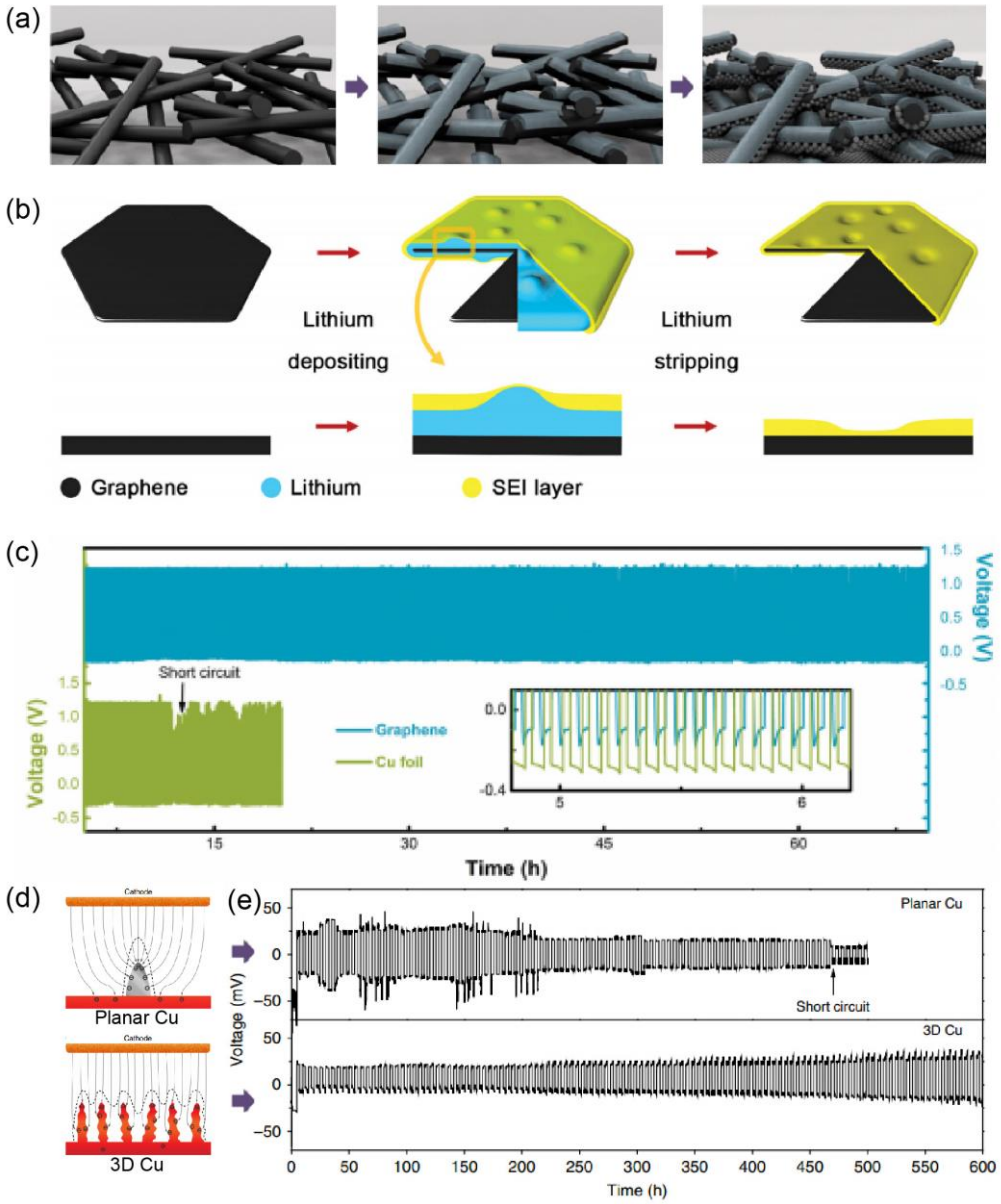

Figure 8. Li metal anode using 3D substrate. a) Structure illustrations of pristine carbon paper, spatially SiC or SiO_2 coated carbon paper, and the Li deposition on this modified carbon paper. Reproduced with permission.[60] Copyright 2012, Elsevier. b) Schematic illustration of unstacked graphene electrode before (left) and after Li plating (middle) and after stripping (right). c) Voltage profiles of Li electrodes on the unstacked graphene or Cu foil at 2.0 mA cm^{-2} with a capacity of 0.1 mAh cm^{-2}. b-c) Reproduced with permission.[61] Copyright 2016, Wiley. d) Illustration of electrochemical Li plating on planar Cu and 3D Cu and e) the corresponding cycling stability of Li on planar Cu and Li in 3D Cu electrodes at 0.2 mA cm^{-2}. d-e) Reproduced with permission.[67] Copyright 2015, Nature Publishing Group.

Although the stability and safety of the Li metal anodes have been significantly improved by adopting the 3D nanostructures, the Li source in those Li metal anodes relies largely on the electrochemical Li deposition. The Li-free substrates could risk Li depletion issues when paired with intercalation cathode materials such as $LiCoO_2$ and $LiFePO_4$. What is worse, the 3D substrates without pre-loaded Li cannot couple with the high-capacity S and O_2 cathodes, which do not contain Li sources. To address these concerns, most recently, pre-loaded Li metal anodes made by thermal infusing Li into the 3D nanostructured host materials have been proposed,[71] which are more attractive and effective for use in batteries, particularly those with non-lithiated cathode materials (S and O_2).

By applying a lithiophilic coating of Si on the porous scaffold (**Figure 9**a-b), molten Li metal can be uniformly coated on the matrix surface or encapsulated inside the 3D structure. It can deliver a large specific capacity up to 2300 mA h g^{-1} as a stable Li metal anode. Due to the minimized effective current density and effective accommodation of Li volume variation, this novel electrode exhibited a stable cycling performance over 80 cycles with smaller overpotential (< 90 mV) at 3 mA cm^{-2}, in sharp comparison with bare Li foil.[71a]

Different from the above random porous structure, the well-aligned channels can guide Li-ion flux move along the vertical direction of the electrode other than the parallel direction, thus inhibiting uncontrolled Li deposition since the flux in each channel is isolated from each other.[51] Very recently, Hu and co-workers proposed a low-tortuosity and channel-guided Li metal anode by adopting carbonized wood (C-wood) as a matrix with pre-loaded Li metal. As shown in Figure 9c, the wetting ability between Li metal and C-wood is improved by the lithiophilic ZnO coating, and afterward, the molten Li can be rapidly infused into and encapsulated within the void space of the C-wood channels (Figure 9d), forming a Li/C-wood electrode. The electrode displays an exceptional cycle stability with a low overpotential (90 mV at 3 mA cm^{-2}) over 225 cycles, indicating that the C-wood channels can serve as an

excellent guide to regulate the Li stripping/plating process and provide good confinement to constrain Li volume change.[71b]

Beside electrically conductive matrixes, Liu *et al*. found that the porous and insulating polyimide membrane can also be infused by molten Li after ZnO coating. Because of the intrinsic electrically insulating feature of polyimide membrane, the infused Li metal itself, instead of the matrix, serves as the electrically conductive media to transport electrons. As a result, the exposed insulating surface after Li stripping will prevent the Li depositing on the top of the matrix directly, thus achieving a surface dendrite-free electrode. The polyimide electrode with pre-loaded Li metal exhibits flat voltage profiles and stable cycling over 100 cycles at a high current density of 5 mA cm^{-2}.[71c]

Instead of using a lithiophilic coating, Lin *et al.* demonstrated that Li can be infused into the nanoscale gaps of layered reduced graphene oxide (rGO) after a spark reaction. The carbonyl and alkoxy groups on the surface of rGO have a strong binding energy to Li, which can promote the infusion of molten Li into the nanogaps of rGO. The process and the corresponding morphology are illustrated in Figure 9e and 9f. The formed Li/rGO anode can deliver a high capacity up to 3390 mAh g^{-1} with an excellent flexibility and small dimensional change (~20%) during cycling. A full cell assembled with $LiCoO_2$ as the cathode and Li/rGO as the anode displays a good rate capability.[71d]

Current studies have demonstrated that rational design of a nanostructured framework for Li metal anode is critical and beneficial to achieve a dendrite-free Li metal anode with improved stability and safety for high-energy-density Li metal batteries. In virtue of the fast-developing nanotechnology, nanostructure engineering of the Li electrode is promised to greatly advance the development of Li metal batteries.

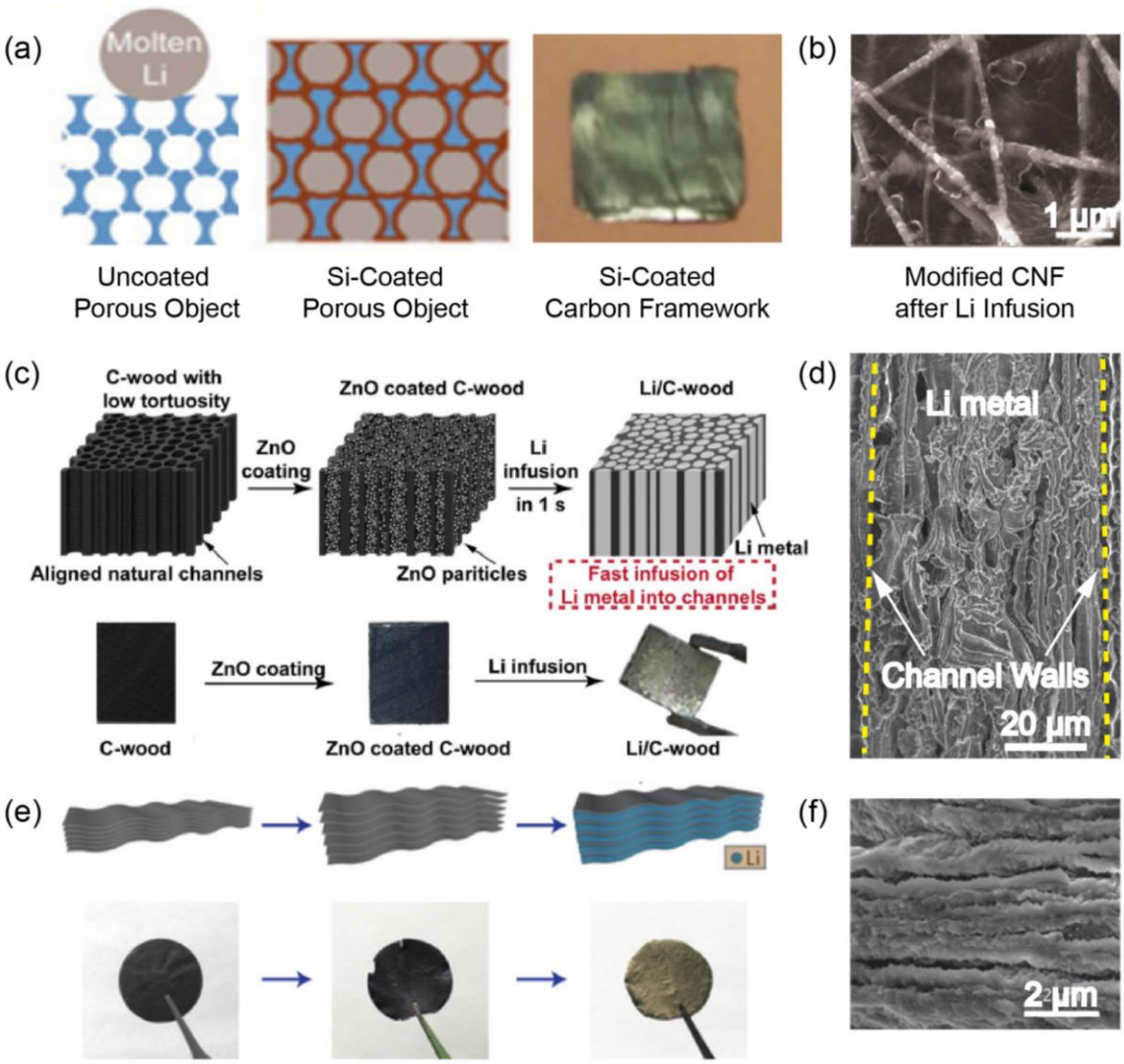

Figure 9. Design of 3D host structure with pre-loaded Li. a) Schematics and digital images of Li infusion into the 3D porous host and b) corresponding SEM image of Li infused in carbon nanofibers (CNF). a-b) Reproduced with permission.[71a] Copyright 2016, National Academy of Sciences. c) Schematics and digital images of the fabrication process from C-wood (left), to ZnO coated C-wood (middle), and finally to Li/C-wood composite (right). d) Cross-sectional view SEM image of the Li metal encapsulated in the C-wood channel. c-d) Reproduced with permission.[71b] Copyright 2017, National Academy of Sciences. e) Schematics and corresponding digital images of GO (left), sparked rGO (middle) and Li-rGO composite. f) SEM image of layered Li-rGO composite. e-f) Reproduced with permission.[71d] Copyright 2016, Nature Publishing Group.

2.4 Separator modification

Generally, the failure of batteries with Li metal anodes stems from the penetration of Li dendrites through the separator. The intense heat release induced by the internal short circuit will further result in a potential explosion hazard. Hence, separator modification has also been considered as a strategy to achieve safe Li metal anodes. The separators are usually modified by surface coating to improve the battery safety.[72] Liu *et al.* also demonstrated that the silica-modified separators can consume the Li dendrites and significantly extend the life of Li metal based batteries up to about five times even when pinholes already exist on the separators (**Figure 10**a). This novel separator displayed a trilayer structure with sandwiched SiO_2 nanoparticles between two inert polymer separators, which can react with Li dendrites that punctured the separator and slow down the growth of Li dendrites (Figure 10b-c).[73]

The small surface area of initial Li deposition and uniform thermal distribution inside the batteries play an important role in improving stability and safety in Li metal anodes. Recently, Luo *et al*.[74] proposed a new approach to address the safety issues by adhering thermally conductive boron nitride (BN) nanosheets to the commercial separators, the bilayer structure of which is shown in Figure 10d. The BN layer can decrease surface area for the initial Li deposition, help facilitate the heat dissipation generated inside the working battery, and create a homogeneous thermal environment (Figure 10e), thus decreasing the risk of dendritic Li growth and improving the cycling stability. Galvanostatic charge/discharge profiles show an improved Coulombic efficiency (92% over 100 cycles at 0.5 mA cm^{-2}) and a stable cycling over 100 cycles at 1.0 mA cm^{-2}.[74]

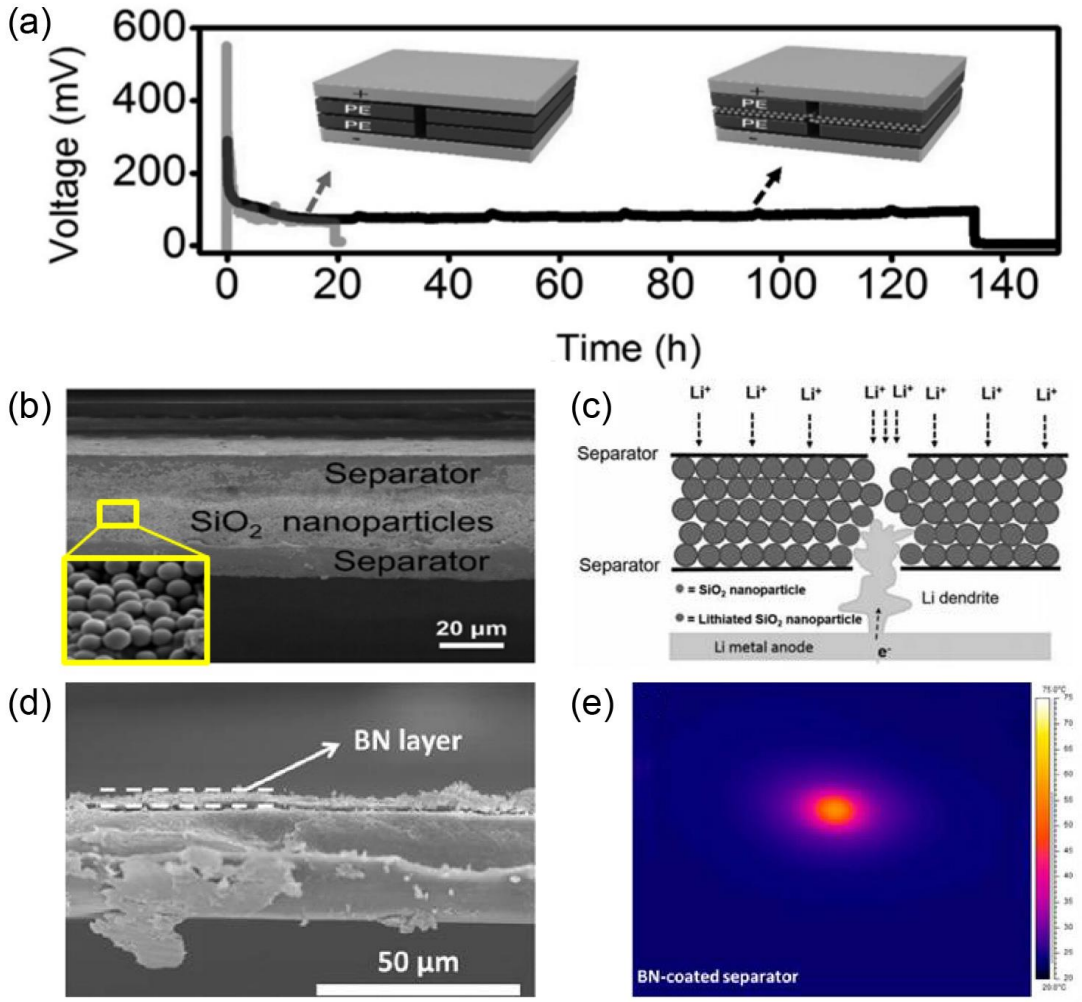

Figure 10. Separator modification for Li anode protection. a) Voltage profiles of a Li/Li cell using a commercial separator (gray) and the trilayer separator (black). b) SEM image of the trilayer separator with silica nanoparticles. c) Mechanism illustration showing a reaction between silica nanoparticles and Li dendrites. a-c) Reproduced with permission.[73] Copyright 2016, Wiley. d) Bilayer structure of BN-coated separator. e) Temperature distribution image of BN-coated separator. d-e) Reproduced with permission.[74] Copyright 2015, American Chemical Society.

As an early detection and warning method, a novel approach has been reported to integrate a bifunctional separator into the batteries to detect Li dendrites in advance.[75] The separator is composed of two inert polymer separators and a metal layer in the middle, a signal of voltage

drop will be detected immediately as soon as Li dendrites connect the anode and the metal layer before causing the internal short-circuit.

3. Li metal anodes with solid-state batteries

The energy densities of Li-ion batteries over the past 25 years are summarized in **Figure 11**a.[76] The state-of-the-art Li-ion batteries have been developed to a volumetric and gravimetric energy density of up to 770 W h L^{-1} and 270 W h kg^{-1}, and these values are approaching a limit. Thus, it is important to adopt Li metal in batteries to further improve the energy density of batteries. Compared to the liquid electrolytes, solid-state electrolytes (SSEs) have good mechanical rigidity and may prevent the Li dendrite. Solid Li batteries using Li metal anodes and SSEs are expected to have higher energy density and better safety. Chemical stability with Li metal anode, interfacial resistance, and processability of the solid electrolytes determine the application of SSEs in Li metal batteries.

SSEs include polymer electrolytes and inorganic solid electrolytes. Figure 11b compares the ionic conductivities of liquid electrolytes, polymer electrolytes, and inorganic SSEs.[76] To practically use SSEs in batteries, several key criteria are required, including high ionic conductivity, good chemical stability with the cathode and Li anode, large electrochemical stability window, good thermal stability, and low electrolyte-electrode interfacial charge-transfer resistance. So far, sulfide/thiophosphate and oxide garnet-type electrolytes are two promising electrolytes for solid batteries.[77] The former one is known for its higher room-temperature conductivities and the latter one is advantageous for its chemical stability against Li metal.

Figure 11c shows the typical battery architectures for the conventional Li-ion and solid-state batteries.[76] As suggested in the schematic, replacing liquid electrolyte with the solid electrolyte while keeping the graphite anode will not increase the volumetric energy density, and conversely, the gravimetric energy density will decrease by 10% because of the high density of solid electrolyte materials compared with the liquid electrolytes. When Li metal is

used to replace graphite anode and solid electrolyte is used, the volumetric and gravimetric energy density will increase by 70% and 40%, respectively. Therefore, it is important to develop solid electrolytes with good Li metal compatibility and apply these SSEs into Li metal batteries for high-energy systems.

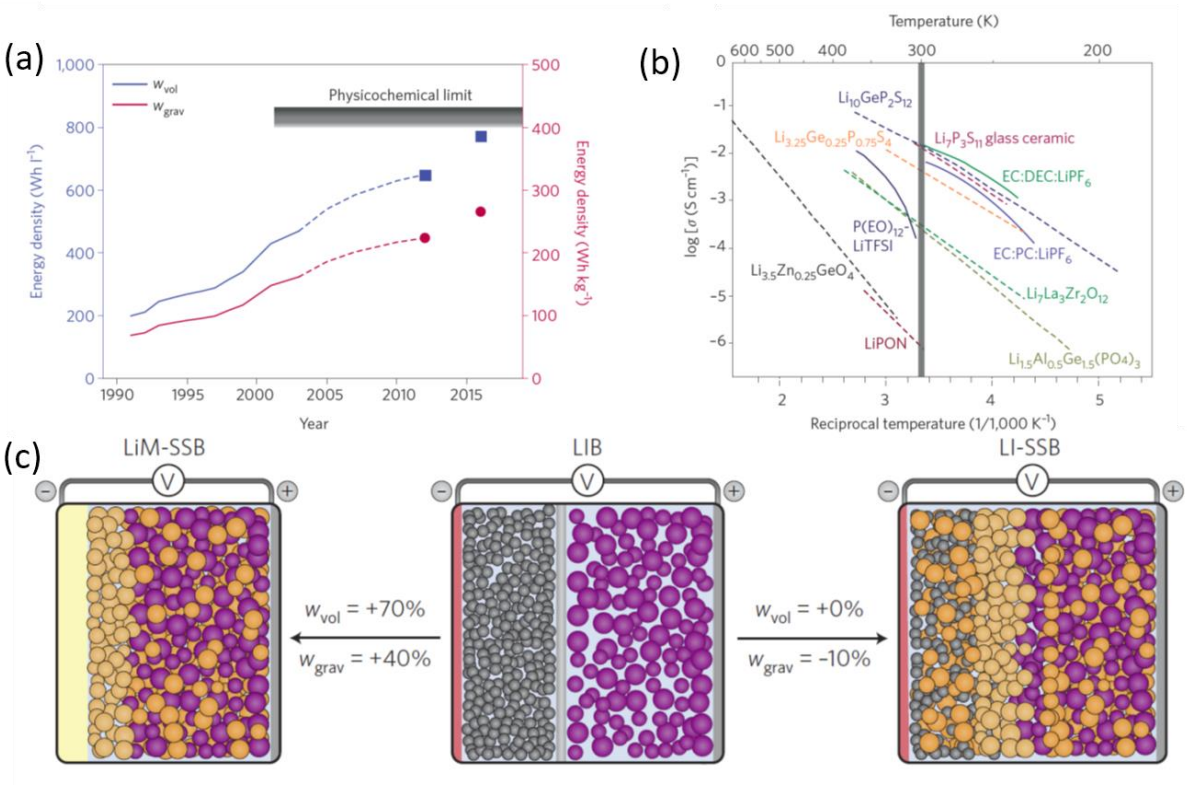

Figure 11. The development of solid Li metal batteries. a) Energy densities and development of lithium-ion batteries. b) Ionic conductivities of various organic electrolytes and SSEs. c) Schematic of battery architectures for the conventional lithium-ion and solid-state batteries using a Li metal anode and a graphite anode. Reproduced with permission.[76] Copyright 2016, Nature Publishing Group.

3.1 Polymer electrolyte

Polymer electrolytes show promise for mechanically suppressing the Li dendrites. Polymer electrolytes based on copolymers, cross-linked polymers, polymer/nanoparticle composites, and so on have been designed to integrate the high ionic conductivity for sufficient Li-ion migration and sufficient shear modulus for Li dendrite formation.[78] A class of polymer

electrolyte known as gel polymer electrolyte combines a polymer network and liquid organic electrolyte. The polymer matrices imbibing organic electrolyte possess high ionic conductivities comparable with those of liquid electrolytes but their mechanical strengths must be enhanced for dendrite-suppressing purposes.

Poly(vinylidene fluoride-co-hexafluoropropylene) (PVDF-HFP) is a widely used polymer matrix for gel polymer electrolyte but has negligible stiffness. Archer and co-workers designed a laminated electrolyte/separator material by sandwiching a nanoporous Al_2O_3 sheet between PVDF-HFP membranes (imbibing 1 M LiTFSI/PC solution).[79] The electrolyte/separator exhibits an ionic conductivity of >1 mS cm^{-1} and mechanical modulus of >0.5 GPa at room temperature, effectively stabilizing Li metal batteries and preventing cell short circuiting. The method incorporating polymer electrolytes with nanostructured ceramics is widely used to enhance the stiffness of the electrolytes for dendrite suppression. SiO_2 hollow nanospheres were employed to provide a mechanically strong scaffold for the gel polymer electrolyte as a composite solid electrolyte with a high ionic conductivity (1.74 mS cm^{-1}) and enhanced safety (non-leakage, low volatility and flammability, and dendrite resistance).[80] Al_2O_3 nanoparticles were used with PVDF-HFP for Li metal protection in the Li-air battery.[81] By constructing a 3D network via a ring-opening polymerization reaction, gel polymer electrolyte can also gain favorable mechanical strength, high ionic conductivity, and low flammability for battery safety.[82]

Among many possible solid polymer electrolytes (SPEs), poly(ethylene oxide) (PEO) based electrolytes are considered as one the most promising candidates owing to the excellent Li-salt solubility and high chain flexibility of PEO.[83] PEO has a good Li-ion solvating ability that the ethylene oxide (EO) functional group can coordinate and form EO-Li^+ complexes, allowing Li ions to hop along PEO long polymer chains. However, the PEO-based SPEs do not have sufficient ionic conductivity at room temperature because of the crystallinity of PEO. At elevated temperature, the conductivity can be improved but the shear modulus of the PEO

is reduced. Various strategies have been employed to improve the ionic conductivity of PEO-based SPEs, such as adding plasticizer or nanofiller, aligning polymer chains, and forming block/grafted copolymer or cross-linking polymers.[83]

For application in Li metal batteries, efforts have also been made to enhance the mechanical properties of SPEs to suppress the growth of Li dendrites. According to a theoretical prediction, the Li dendrite problem would be eliminated if the shear modulus (G) of the separator/electrolyte exceeds twice that of Li metal (i.e., $G > 2\ G_{Li}$, or $G > 6$ GPa at room temperature).[41] Recently, an interpenetrating network of poly(ether-acrylate) SPE has been reported by photopolymerization of PEO and branched acrylate. The interpenetrating poly(ether-acrylate) SPE integrates both exceptional mechanical strength (~12 GPa) and high ionic conductivity (2.2×10^{-4} S cm^{-1} at room temperature). Therefore, it can suppress the dendrite growth and facilitate the Li-ion migration for favorable Li metal plating/stripping. However, Archer *et al.* pointed out that the criterion, $G > 2G_{Li}$ is not necessarily a requirement for inhibiting Li dendrite growth.[84] They designed an SPE composed of stiff polyethylene (PE) cross-linked by PEO segments.[85] As illustrated in **Figure 12**a, the crystallinity of PEO is reduced by the PE backbones, resulting in improved ionic conductivity (Figure 12b). By tuning the amount of poly(ethylene glycol) (PEG, oligomer of ethylene oxide) in the cross-linked PE-PEO, the cross-linked plasticized SPE with 39 wt.% PEG exhibits a high ionic conductivity of 2.0×10^{-4} S cm^{-1} at 25 °C. The dendrite-resisting effect of the PE-PEO SPEs is demonstrated by test the charge (C_d) passed the cell at different current densities before cell failure induced by Li dendrite short-circuits. The cross-linked SPEs increase the lifetime of the Li metal cells (indicated by C_d) by over an order of magnitude that of PEO, implying the exceptional dendrite-resisting capability of the PE-PEO SPEs, despite their modest shear moduli (10^5 Pa at 90 °C, much lower than G_{Li}). The excellent ionic conductivity and Li dendrite growth resistance are attributed to the nanoporous

network in the polymer, which can facilitate the migration of Li ions while precluding the proliferation of the microscale Li dendrites.

Pan *et al*. reported another cross-linked SPE using polyhedral oligomeric silsesquioxane (POSS) cross-linked PEG to inhibit Li dendrite problems, which is schematically presented in Figure 12d.[86] The POSS particles provide essential mechanical strength for the cross-linked polymer electrolyte while the PEG chains solvate the Li ions for ion conduction. The modulus and ionic conductivity of the polymer electrolyte are optimized by changing the molar ratio (*n*) of POSS to PEG and PEG molecular weight (*m*) in POSS-*n*PEG*m*. The ionic conductivity increases with the POSS/PEG ratio (Figure 12e). At 105 °C, POSS-4PEG2K has a high conductivity of >1 mS cm^{-1} while maintaining a modulus of 33.6 MPa. Although the moduli of the POSS-*n*PEG*m* electrolytes do not meet the modulus criterion to mechanically prevent Li dendrite growth (G > 6 GPa, room temperature), the cross-linked polymer electrolytes are demonstrated to be effective at blocking Li dendrites and improving the cell life. The symmetric cell using POSS-4PEG2K can run stably at 0.3 mA cm^{-2} for 2600 h (C_d > 2808 C cm^{-2} Figure 12f), which is 50 times that of the PEO control cell. The results demonstrate the exceptional ability of the cross-linked polymer electrolyte to suppress the growth of Li dendrite.

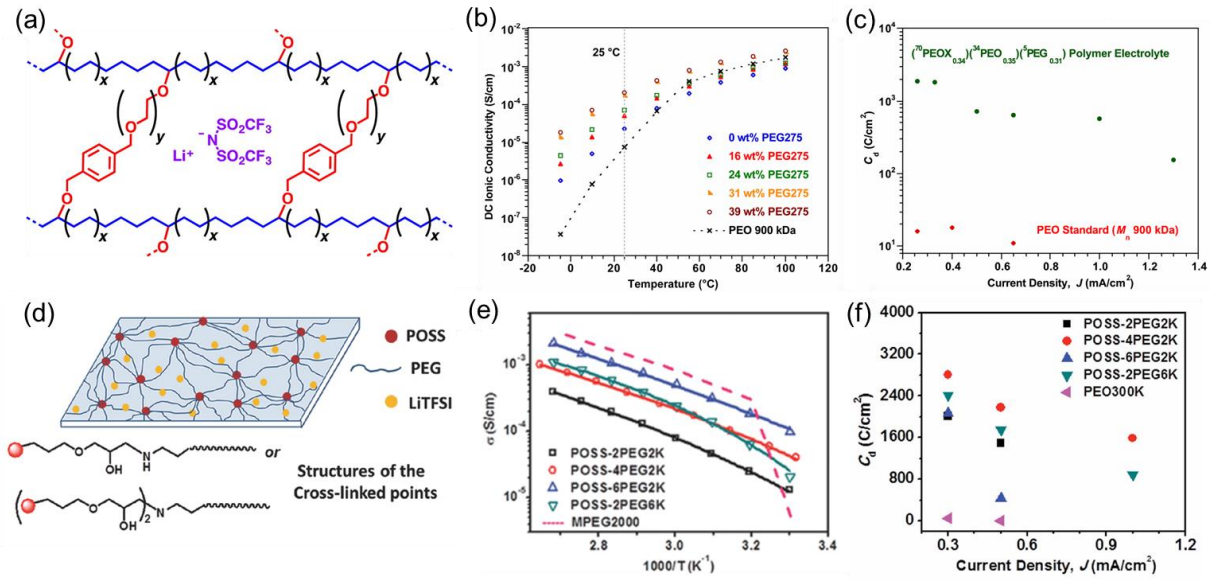

Figure 12. Cross-linked solid-state polymer electrolytes for Li metal anodes. a) Schematic of cross-linked polyethylene-poly(ethylene oxide) (PE-PEO) SPE. b) Ionic conductivity of the PE-PEO cross-linked SPEs with different ratios. c) Total charge passing the cell before cell failure (C_d) at 90 °C for PE-PEO polymer electrolyte and PEO standard. a-c) Reproduced with permission.[85] Copyright 2014, American Chemical Society. d) Schematic presentation of the cross-linked POSS-PEG hybrid polymer electrolyte on Li metal anode to block Li dendrites. e) Ionic conductivity (σ) of POSS-*n*PEG*m* at different temperatures. f) C_d at different current densities in the Li symmetric cells using POSS-*n*PEG*m* polymer electrolytes. d-f) Reproduced with permission.[86] Copyright 2015, Wiley.

3.2 Polymer-inorganic composite electrolytes

In polymer electrolytes, fillers can change the local crystalline structure of polymer to an amorphous state, causing reorient neighboring polymer chains to reorient and create liquid-like Li^+ diffusion. In addition, the fillers can enlarge the electrochemical stability window and increase elastic modulus of solid polymer electrolytes. Previous studies have reported to use different fillers to improve the performance of PEO polymer-based composite electrolytes. Fillers include passive inorganic nanoparticles (non-conductive for Li-ions) such as Al_2O_3, SiO_2, TiO_2, ZrO_2, active nanoparticles such as $Li_{0.33}La_{0.557}TiO_3$, $Li_{1.3}Al_{0.3}Ti_{1.7}(PO_4)_3$, and organic polymer nanoparticles.[87] The nano-sized inorganic particles in the polymer-inorganic composite electrolytes can significantly decrease the crystallinity of polymers and increase the surface area of the amorphous region. For example, Cui and co-workers reported a PEO electrolyte with in-situ synthesized and monodispersed ultrafine SiO_2 nanospheres, which shows high ionic conductivity (4.4×10^{-5} S cm^{-1} at 30 °C and 1.2×10^{-3} S cm^{-1} at 60 °C).[87c] In a recent study, researchers found that the ionic conductivity of PEO electrolyte containing active nanoparticles is 1 to 2 orders of magnitude higher than that of polymer matrix and is also higher compared to the polymer matrix containing passive nanoparticles. Such

enhancement is attributed to a pronounced restructuring within the interface around the particles; when polymer and active fillers share a common component, there exists a driving force to balance the chemical potential of lithium between both phases.[88]

Introducing active nanowire or nanofiber networks in polymer matrices are effective ways to increase the ionic conductivity of polymer-inorganic composite electrolyte. Compared to the isolated nanoparticles, the nanowire and nanofiber networks can provide extended ionic transport pathways in the polymer matrix. Cui and co-workers developed one-dimensional $Li_{0.33}La_{0.557}TiO_3$ nanowires as Li-ion conductive fillers in the composite electrolyte (**Figure 13**a).[89] They used ceramic nanowires to facilitate ion conduction networks in the polymer electrolyte. The electrolyte exhibits an ionic conductivity of 2.4×10^{-4} S cm^{-1} at room temperature with 15 wt.% of $Li_{0.33}La_{0.557}TiO_3$ nanowires in polyacrylonitrile/$LiClO_4$. The improvement of the ionic conductivity can be explained by the concentrated Li ions on the $Li_{0.33}La_{0.557}TiO_3$ nanowire surface caused by the strong complexation between ClO_4^- and acidic groups on $Li_{0.33}La_{0.557}TiO_3$ that dissociates $LiClO_4$ and forms a fast pathway for Li diffusion. In the following work, Cui and co-workers used Y_2O_3-doped ZrO_2 (YSZ) nanowires with positively charged oxygen vacancies on the surface to design improved ionic conductivity in the composite polymer electrolyte.[90] The positively charged oxygen vacancies can associate with anions of salt to release Li ions and a continuous fast conduction pathway can be created by nanowires, which is unattainable with nanoparticles (Figure 13b and 13c).

To avoid agglomeration of individual isolated fillers, Hu and co-workers recently developed a 3D garnet-type $Li_{6.4}La_3Zr_2Al_{0.2}O_{12}$ (LLZO) nanofiber networks to enhance the ionic conductivity of dry polymer electrolyte.[91] The garnet-type ceramic electrolyte is selected for its high ionic conductivity and good chemical and electrochemical stability. As shown in Figure 13c, the LLZO consists of interconnected nanofibers and these nanofibers form a continuous Li-ion transport network. This design does not need to mechanically mix the

fillers and avoids their agglomerations in the polymer matrix. The schematic fabrication of the solid electrolyte is shown in Figure 13d. The garnet LLZO nanofibers were prepared using electrospinning technique. Garnet LLZO salts and sacrificial polymer were mixed and electrospun into to a nanofiber membrane, followed by sintering at 800 °C in air to obtain the garnet ceramic nanofiber networks. PEO/Li salt was then infiltrated into the 3D ceramic networks to form the solid composite electrolyte membrane. The SEM image in Figure 13e shows the interconnected garnet nanofibers. Figure 13f shows the cross-section of the solid electrolyte membrane with a thickness of 40-50 µm. Conventionally, polymer electrolytes are built on their own polymer structure for which there is no mechanical support to ensure the structural stability. When temperature increase, the flow of polymers may squeeze cathode and anode and their contact will lead to short circuit. The garnet nanofiber-based solid composite electrolyte can avoid such safety concerns. As shown in Figure 13g, the garnet nanofiber provides a fire-retardant property, which shows a good mechanical support for polymer electrolyte. The garnet nanofiber based solid electrolyte has an ionic conductivity of 2.5×10^{-4} S cm^{-1} at room temperature (Figure 13h). The long-term cycling stability of the symmetric Li-electrolyte-Li cell at a current density of 0.5 mA/cm^2 indicates good electrochemical stability with long cycle life (Figure 13i).

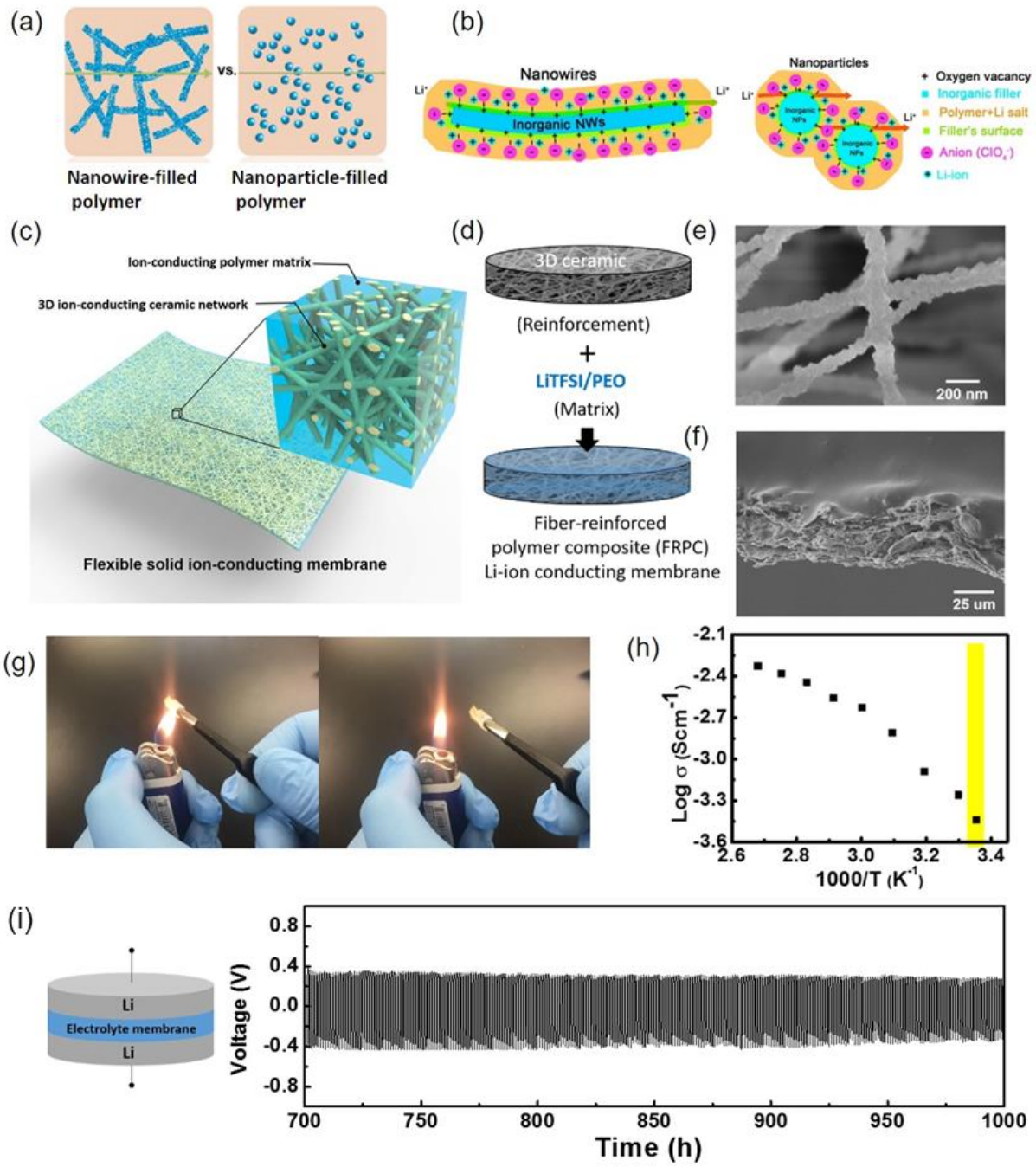

Figure 13. Composite electrolytes using inorganic fillers and solid polymer electrolytes. a) Schematic of nanowire and nanoparticle fillers in the polymer matrix. Reproduced with permission.[89] Copyright 2015, American Chemical Society. b) Mechanism of ion transport in nanowire-filled and nanoparticle-filled polymer electrolytes. Reproduced with permission.[90] Copyright 2016, American Chemical Society. c) Schematic of nanofiber network in the polymer electrolyte. d) Schematic of preparation of fiber-reinforced polymer composite electrolyte. e) SEM images of garnet nanofibers and f) cross-section of the electrolyte

composites. g) Flammability demonstration of the solid composite electrolyte indicating its thermal stability. h) Ionic conductivity of polymer composite electrolyte at elevated temperatures. i) Li stripping/plating of Li/polymer electrolyte/Li cell, demonstrating good electrochemical stability of polymer electrolyte. c-i) Reproduced with permission.[91] Copyright 2016, National Academy of Sciences

3.3 Inorganic solid-state electrolytes

3.3.1 Li-SSE interface stability

Inorganic SSEs are crystalline, glass, or ceramic materials, and are single ion conductors with Li-ion transfer number of ~1, which allow only Li-ion transfer. Mo and co-workers have conducted a computational study on the interface stability between the solid electrolytes and Li metal anodes.[92] Based on the simulation work, inorganic SSE materials are not thermodynamically stable with metallic Li and tend to be reduced at low voltages with highly favorable decomposition energy, as shown in **Figure 14**a and 14b.[92] The decomposition energy indicates the favorable reaction between the solid electrolyte and Li metal. Figure 14a shows the decomposition energy of sulfide SSE materials as a function of voltage. For example, $Li_{10}GeP_2S_{12}$ (LGPS) will be reduced by Li below 1.7 V and has a decomposition energy of -1.25 eV/atom at 0 V. At the equilibrium state at 0 V, LGPS will be decomposed to form $Li_{15}G_4$, Li_3P, and Li_2S.[92-93] Other sulfides materials, such as $Li_{3.25}Ge_{0.25}P_{0.75}S_4$, Li_3PS_3, Li_4GeS_4, Li_6PS_5Cl, and $Li_7P_2S_8I$, can be reduced by Li metal in a similar voltage range (~1.6–1.7 V). The decomposition energy decreases with the potential to approximately −1 eV/atom at 0 V, suggesting highly favorable reduction reactions of the sulfide solid electrolytes. The highly favorable reaction indicates that sulfide SSEs are not stable with Li and in battery design; thus, they cannot contact with Li metal directly. In Figure 14b, oxide solid electrolyte materials have different decomposition potentials. $Li_{0.33}La_{0.56}TiO_3$ (LLTO) and $Li_{1.3}Ti_{1.7}Al_{0.3}(PO_4)_3$ (LATP) will reduce at low voltages during which Ti^{4+} in LLTO and

LATP is converted to Ti^{3+} or lower valences. Ge-containing oxide electrolyte materials, such as $Li_{1.5}Al_{0.5}Ge_{1.5}(PO_4)_3$ (LAGP) and $Li_{3.5}Zn_{0.25}GeO_4$ (i.e., LISICON), can be reduced as well due to the formation of Li-Ge alloy at low voltages.

Among the oxide solid electrolytes, garnet-type $Li_7La_3Zr_2O_{12}$ (LLZO) has the lowest reduction potential of 0.05 V versus Li^+/Li and the least favorable decomposition reaction energy. Given the small reaction potential, reduction of LLZO may be kinetically inhibited and their reduction products, such as Li_2O, Zr_3O, and La_2O_3, may work as passivation layers to protect LLZO electrolyte from further decomposition. The electrochemical stability windows of various solid electrolyte materials are shown in Figure 14c and the oxidation potentials required to completely delithiate the electrolyte material are marked by the dash line. It shows that Li binary compounds, including LiF, Li_2O, Li_2S, Li_3P, and Li_3N are thermodynamically stable with Li. With these compounds at the Li-electrolyte interface, the interface may be stabilized against Li metal beyond the reduction potential limit of the solid electrolytes (Figure 14d). The Li chemical potential is the sum of the ionic carrier and electronic carrier. The electrochemical potential of the ionic carrier is constant across the interface but the electronic carrier decreases at the interface. Thus, the decomposition has no thermodynamic driving force to favor reaction in the bulk. Therefore, a passivation layer at the interface can decrease the Li chemical potential applied on the solid electrolyte and help to bridge the Li chemical potential gap between Li and solid electrolytes. LiPON, Li_3PS_4, and $Li_7P_2S_8I$ can form a passivation layer at the interface and experimentally exhibit good Li metal compatibility.

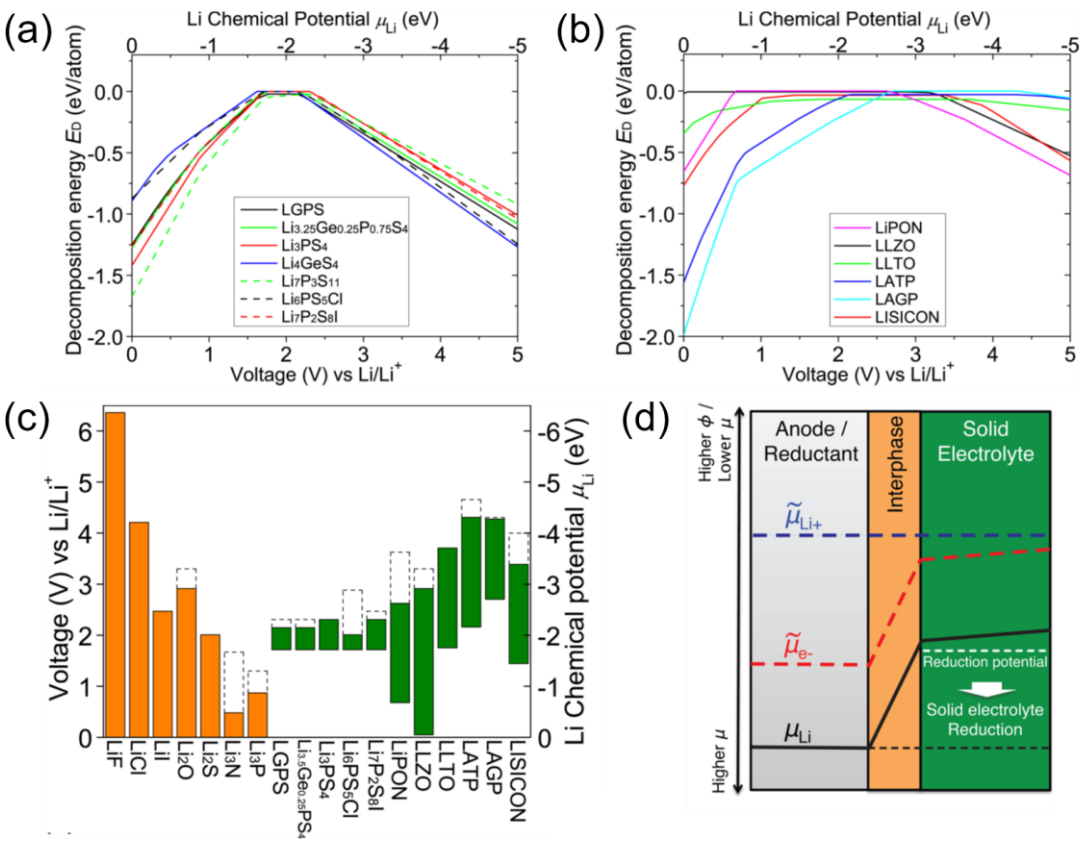

Figure 14. Computational study on the Li-SSE interface stability. Decomposition energy E_D of a) sulfide and b) oxide solid electrolyte materials as a function of the applied voltage ϕ or Li chemical potential μ_{Li}. c) Electrochemical window (solid color bar) of the solid electrolyte and other materials. The oxidation potential for complete delithiation is marked by the dashed line. d) Schematic diagram of the change of Li chemical potentials μ_{Li} (black line), the electrochemical potential $\tilde{\mu}_{Li+}$ (blue dashed line), and $\tilde{\mu}_{e-}$ (red dashed line) at the Li-electrolyte interface. Reproduced with permission.[92] Copyright 2015, American Chemical Society.

Since sulfide/thiophosphate are not thermodynamically stable with Li metal, protecting interface is important to stabilize the electrolyte/electrode contact.[94] Liang and co-workers reported using a Li-compatible composite to chemically passivate the surface of the SSE. They applied $3LiBH_4 \cdot LiI$ (LB-LiI) as the passivation material.[94a] Since sulfide electrolyte is not stable with metallic Li, the symmetric cell has a noisy voltage plateau, indicating a poor interface stability. When LB-LiI was applied at the interface, the symmetric cell had a smooth and stable voltage, indicating a stable interface and a high electrochemical stability.[94a]

3.3.2 Li alloy for Li-SSE interface wettability

Oxide garnet-type SSEs ($Li_7La_3Zr_2O_{12}$ and analog) are promising electrolytes for solid Li metal batteries. Extensive studies have been conducted to further improve their ionic conductivity, enhance their chemical stability against Li metal, and decrease their interfacial resistance with Li.[95] The high interfacial resistance of the SSE and Li metal is one of the main challenges that haunted solid Li metal batteries for years.[96] To reduce the interfacial resistance, the electrolytes should have stable and good contact with the Li metal. Tailoring chemical compositions, applying external pressure to improve physical contact, and heating Li metal have been reported to reduce the interfacial resistance between the garnet solid electrolyte and Li metal.[97]

The poor wettability of the Li metal on the garnet causes microscopic gaps at the interface, leading to an intrinsically high impedance. Recently, Hu and co-workers reported that introduction of Al_2O_3 coating can improve the wettability and stability of Li metal against garnet by forming a Li-Al-O at the interface.[98] The Li-Al-O alloy is Li-ion conductive and electron insulating, leading to a stable interface. **Figure 15**a shows the schematic of the garnet SSE and Li interface. The macroscopic gaps suggest a poor contact between garnet SSE and Li. Using ALD coating, the Al_2O_3 can help the molten Li form conformal coating on the garnet surface. SEM images in Figure 15b compares the morphology of garnet SSE and the Li metal interface. Without ALD coating, the physical gap can be clearly observed. These gaps directly result in high interfacial resistance up to ~10^3 Ω cm^2. With ALD coating, the reaction of Al_2O_3 with molten Li provides the driving force for conformal contact with each other. The total impedances before with and without Al_2O_3 coating are shown in Figure 15c. The calculated interfacial impedance is decreased from 1710 to 34 Ω cm^2. The Li symmetric garnet cell with Al_2O_3 was stabilized at ~13 mV at a current density of 0.1 mA/cm^2, whereas the cell without Al_2O_3 exhibited a noisy potential (Figure 15d). The low interfacial impedance and good interface of garnet electrolyte and Li metal enable a high-voltage Li metal battery as

schematically shown in Figure 15e. The full cell is assembled based on the Li/Al_2O_3-garnet and $Li_2FeMn_3O_8$ cathode. A small amount of high-voltage liquid electrolyte was used in the cathode to wet the garnet-cathode interface and the working cell successfully powered a light emitting diode (LED) (Figure 15f).

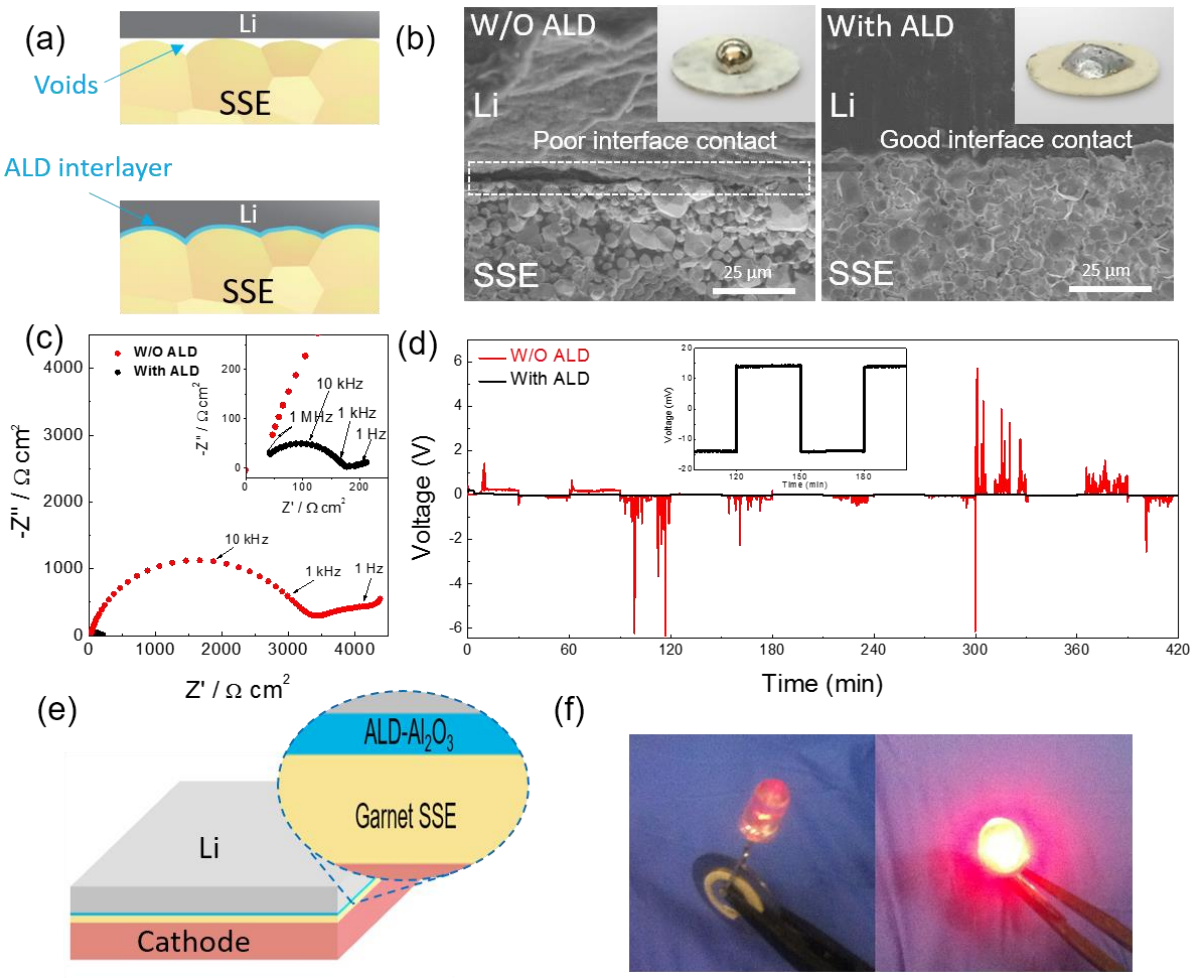

Figure 15. Interface of garnet SSE and Li metal anode. a) Schematic of the interface between of garnet surface and metallic Li. b) SEM images of the garnet solid electrolyte/Li metal interface. Insets are photos of a drop of molten on garnet disk. c) EIS profiles of the symmetric Li/garnet cells with and without ALD coating. Inset shows the enlarged impedance curve of the ALD treated garnet cell. d) DC cycling of Li/garnet symmetric cells at a current density of 0.1 mA cm^{-2}. The inset is the magnified curve of the ALD-garnet cell. e) Schematic of full cell based on garnet/Li configuration. f) A working cell to light up an LED device. Reproduced with permission.[98] Copyright 2017, Nature Publishing Group.

Introducing a secondary phase to react with Li metal is a straightforward and effective way to improve the wettability of the SSEs with Li. The secondary phase can react with molten Li to form a Li-rich alloy, and this reaction will provide a driving force to coat Li metal conformally on the SSE surface and change the wettability of SSE from lithiophobic to lithiophilic. Recently, Au, Si, and ZnO have been applied to engineer the interface of garnet/Li interface.[99] Tsai *et al*. reported to use a thin Au buffer layer to improve the contact of the garnet SSE and the Li electrodes.[99a] As schematically shown in **Figure 16**a, Li dendrite would form because of the inhomogeneous contact between the SSE and Li electrodes. Using Au buffer layer, the total resistance of the Li symmetric solid electrolyte cell is dramatically reduced from 3000 to 380 Ω cm^2, suggesting an improved interfacial contact (Figure 16b). The motivation of using Au buffer layer is that Au and Li can form an alloy at room temperature, and it can provide a good contact with the solid electrolyte and help to redistribute the Li dissolution and deposition. Inspired by this work, following research based on Si and ZnO_2 has been reported. An ultrathin (~10 nm) layer of amorphous Si was coated onto garnet electrolyte by chemical vapor deposition method to form a conformal coating, followed by reacting with molten Li.[99b] As shown in Figure 16c, Si was selectively coated on half of garnet pellet and the brown color indicates the Si-coated area. By dipping into molten Li in a short time (~4 s), the garnet with Si was fully coated by Li and the other side without Si remained clean, indicating that Si layer transformed the garnet from lithiophobic to lithiophilic. The Nyquist plots of the Li|garnet|Li cells exhibited a dramatic impedance and the interfacial resistance decrease from 925 to 127 Ω cm^2 (Figure 16d). ZnO is another active material that can react with molten Li to form a Li-Zn alloy at the interface, which is schematically shown in Figure 16e.[99c] Molten Li can diffuse fast in the ZnO coating layer to enable good Li contact with the garnet solid electrolyte and markedly reduce interfacial resistance (Figure 16f).

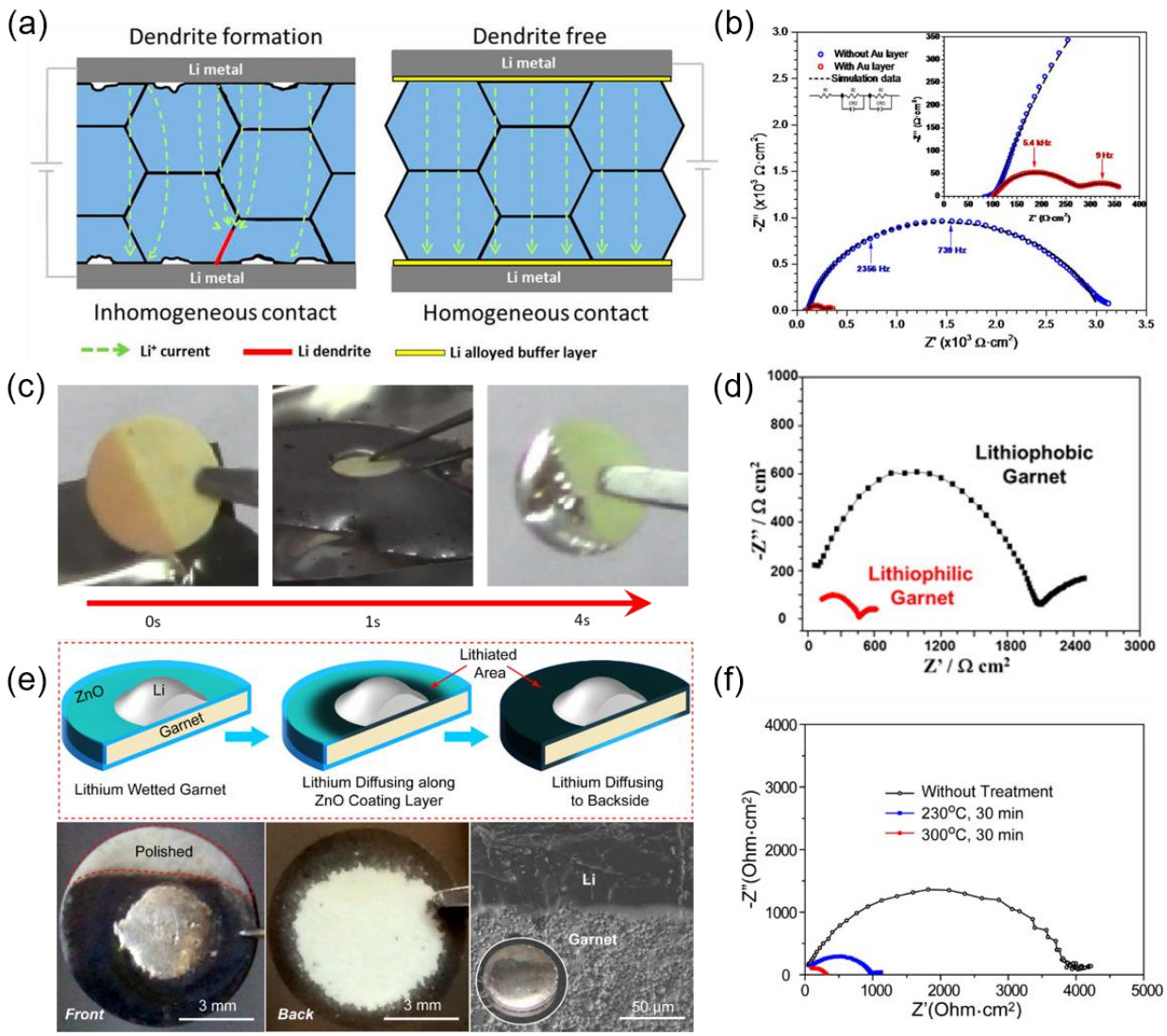

Figure 16. Li-SSE interface wettability improvement via Li alloys. a) Garnet/Li interface using an Au buffer layer to improve its interfacial contact. b) EIS of the Li symmetric cell with and without Au. a-b) Reproduced with permission.[99a] Copyright 2016, American Chemical Society. c) Li melting-diffusion experiment images on half-coated garnet showing the Li wettability on the garnet with or without Si modification. d) EIS of the Li symmetric cell with and without Si. c-d) Reproduced with permission. [99b] Copyright 2016, American Chemical Society. e) Schematics, digital photos and SEM images showing the wettability of garnet-Li interface using ZnO coating layer. f) EIS of the Li symmetric cell with and without ZnO. e-f) Reproduced with permission.[99c] Copyright 2017, American Chemical Society.

3.3.3 Interface engineering

Designing an engineered interface is another way to decrease the interface resistance between the electrode and the SSEs. Rupp and co-workers developed a porous interface on garnet electrolyte pellet. By contacting and embedding active materials in the porous structure, the interfacial resistance was decreased.[100] **Figure 17**a compares a flat interface and a porous interface between electrode and electrolyte. The interface was engineered by employing a sacrificial organic template on a dense solid electrolyte pellet, followed by sintering to remove the organic template. The slurry consisting of $Li_4Ti_5O_{12}$, conductive carbon, and polymers was cast onto the flat or porous structure. Cross-section of two types of interfaces is compared and shown in SEM images of Figure 17b. In the non-modified battery, an obvious interface can be observed, where the poor contact results in a high impedance (Figure 17c). In the interface-engineered battery, the electrode layer is intimately embedded in the porous layer of solid electrolyte, and no division line is observed. The increased contact area of electrodes and electrolyte directly leads to a reduced impedance in the EIS profile (Figure 17c). This work displays the importance of engineering the interfacial structure between electrodes and solid electrolytes. More efforts should be placed on the development of interface-engineered structures and construction of solid-state electrolyte frames to host electrodes with improved contact areas.

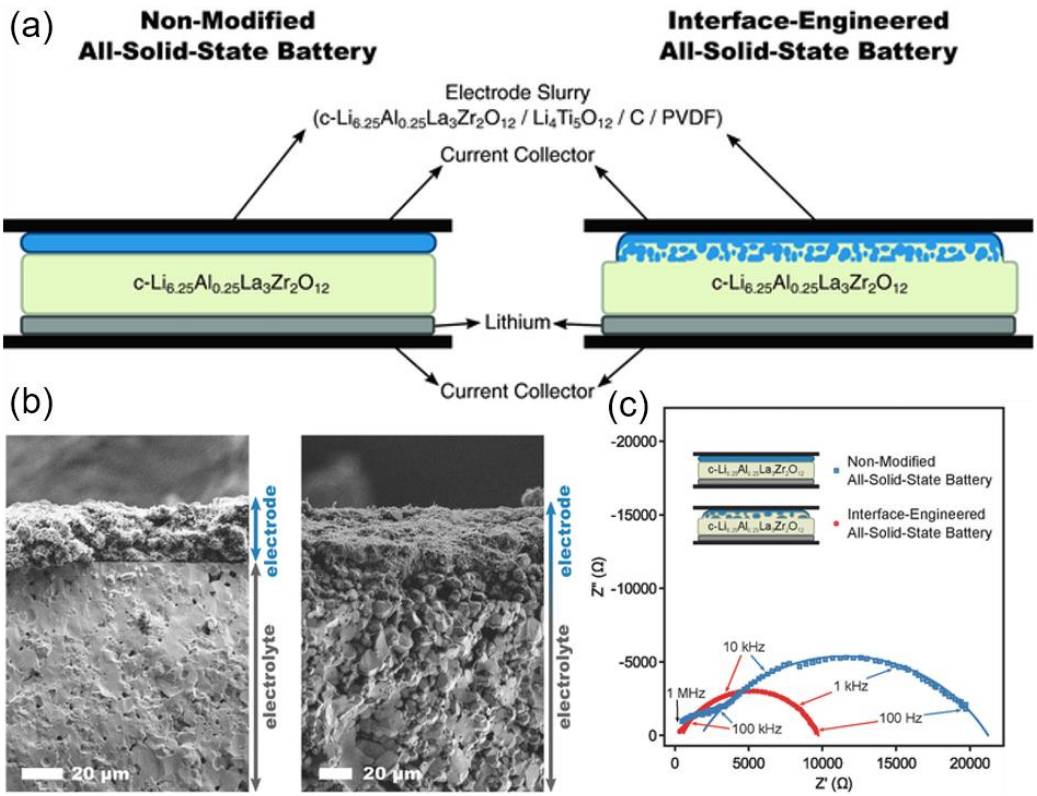

Figure 17. Nanoengineering on SSE for interface contact. a) Schematic of a non-modified solid-state battery and interface-engineered solid-state battery. b) SEM images of cross-sectional interfaces of electrolyte and electrode for non-modified and interface-engineered pellets. c) Nyquist plots of the non-modified and interface-engineered batteries. Reproduced with permission.[100] Copyright 2016, Wiley.

3.3.4 Polymer interface modification for inorganic SSEs

Adding a polymer interface between the SSE and the metal anode is an effective way to decrease the interfacial resistance.[101] Polymer interlayer can suppress Li dendrite nucleation due to the uniform Li-ion flux and good wettability with Li metal. Goodenough and co-workers have recently reported a design of hybrid polymer/ceramic/polymer sandwich electrolyte for Li metal batteries. **Figure 18**a gives the schematic of the hybrid solid-state battery design.[101d] In this work, cross-linked poly(ethylene glycol) methyl ether acrylate was selected as the polymer. The polymer structure is shown in Figure 18b. In the 3D polymer structure, the side chain on the polyacrylate framework can facilitate Li-ion transfer. The

polymer has a high melting temperature (~270 °C), which contributes to a good thermal stability to remain solid in the Li metal battery at working temperature (65 °C). Compared with the conventional single polymer electrolyte in batteries, the polymer/ceramic/polymer hybrid electrolyte can reduce the magnitude of the electric field across the interface and stabilize the polymer electrolyte. As indicated in the schematic of Figure 18c, charge carriers will redistribute in both phases and create an electric double layer at the interface. Because the ceramic electrolyte can block the anion of the salt in the polymer, the Li ionic transfer number will be decreased and the positive charges trapped at the interface will be decreased. In the single polymer electrolyte, a stronger interface electric field may cause chemical reactions at the interface of polymer and Li metal, leading to cycling performance decay and Coulombic efficiency decrease.

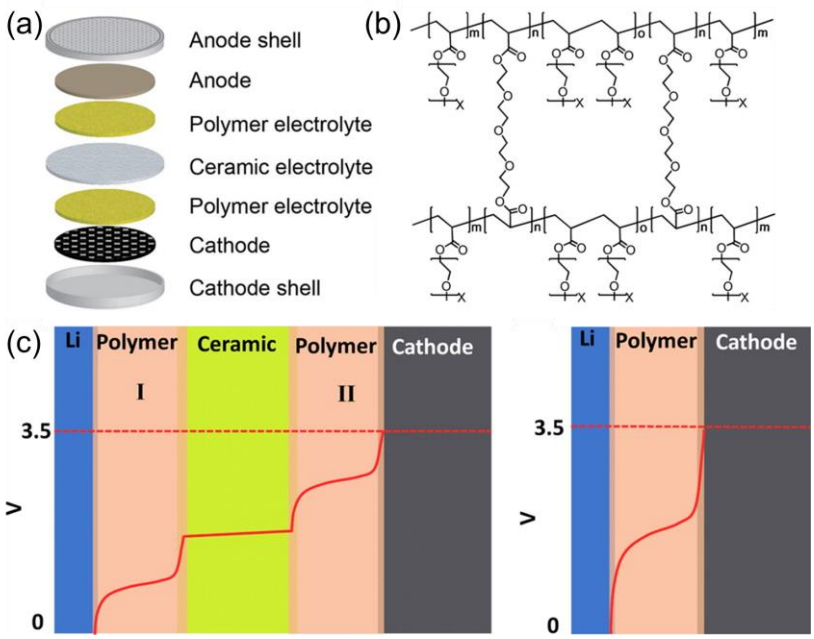

Figure 18. Polymer-inorganic hybrid electrolyte in Li metal battery. a) Schematic of full cell configuration using polymer/ceramic/polymer sandwich electrolyte to improve the interface. b) Structure of cross-linked poly(ethylene glycol) methyl ether acrylate as the polymer electrolyte. c) Illustration of the electric potential profile across the sandwich electrolyte and individual polymer electrolyte in the charge process of a cell. Reproduced with permission.[101d] Copyright 2016, American Chemical Society.

3.3.5 Liquid-solid hybrid electrolyte systems

In addition to using the solid polymer electrolyte as an interlayer, liquid electrolytes can help to decrease the interfacial resistance. Extensive studies have been carried out to understand the interface chemistry between the solid electrolyte and liquid electrolyte and their compatibility in full cells.[102] In the binary liquid-solid electrolyte system, LAGP, LATP, and LISICON have been reported as the solid electrolyte. Hagen and co-workers reported the use of polymer separator wetted by liquid organic solvent as an interlayer to improve the interface between the electrode and solid electrolyte.[102a] Wen and co-workers applied $Li_{1.5}Al_{0.5}Ge_{1.5}(PO_4)_3$ as a separator to fabricate hybrid electrolyte Li-S battery.[102b] Conventional Li-S electrolyte (LiTFSI in DME/DOL) was filled in the space between solid electrolyte and electrodes. The schematic of the battery configuration is shown in **Figure 19**a. In this design, the inorganic solid electrolyte can prevent the soluble polysulfides and suppress the formation of Li dendrite. Later, Xia and co-workers developed a hybrid battery based on a LISICON type $Li_{1+x+y}Al_xTi_{2-x}Si_yP_{3-y}O_{12}$ (LATP) solid electrolyte.[102c] Two different types of electrolytes were used. In the cathode side, $LiClO_4$ in THF was used and Li_2S was dispersed in it. In the anode side, $LiPF_6$ in EC/DMC/DEC was used. Manthiram and co-workers used LISICON type $Li_{1.3}Al_{0.3}Ti_{1.7}(PO_4)_3$ electrolyte to fabricate a hybrid cell (Figure 19c).[102d] Dissolved Li_2S_6 catholyte was used as the cathode. These studies have shown a great improvement in the capacity and Coulombic efficiency of the Li-S battery, but a detailed understanding of interface stability between the liquid organic electrolyte and solid electrolyte remains unclear.

Recently, Janek and co-workers studied the interface between the liquid electrolyte and LAGP solid electrolyte, revealing that a resistive solid-liquid electrolyte interface (SLEI) can be formed at the interface. Figure 19d shows the schematic of ion transport and resistance contribution in cells with solid-liquid phase boundaries.[102e] In the interfaces between solid and liquid electrolytes, the ion conduction mechanism changes from the diffusion of solvated

ions in liquid electrolytes to a hopping mechanism in solid electrolytes. The transport of ions across the phase boundary and the SLEI contribute to the overall impedance.[102e] Their study shows that the SLEI contains inorganic compounds originate from decomposition products of the conducting salt and probably from the solid electrolyte, but also organic and polymer compounds. This SLEI can grow to a finite thickness and will reach a threshold of the resistance contribution.

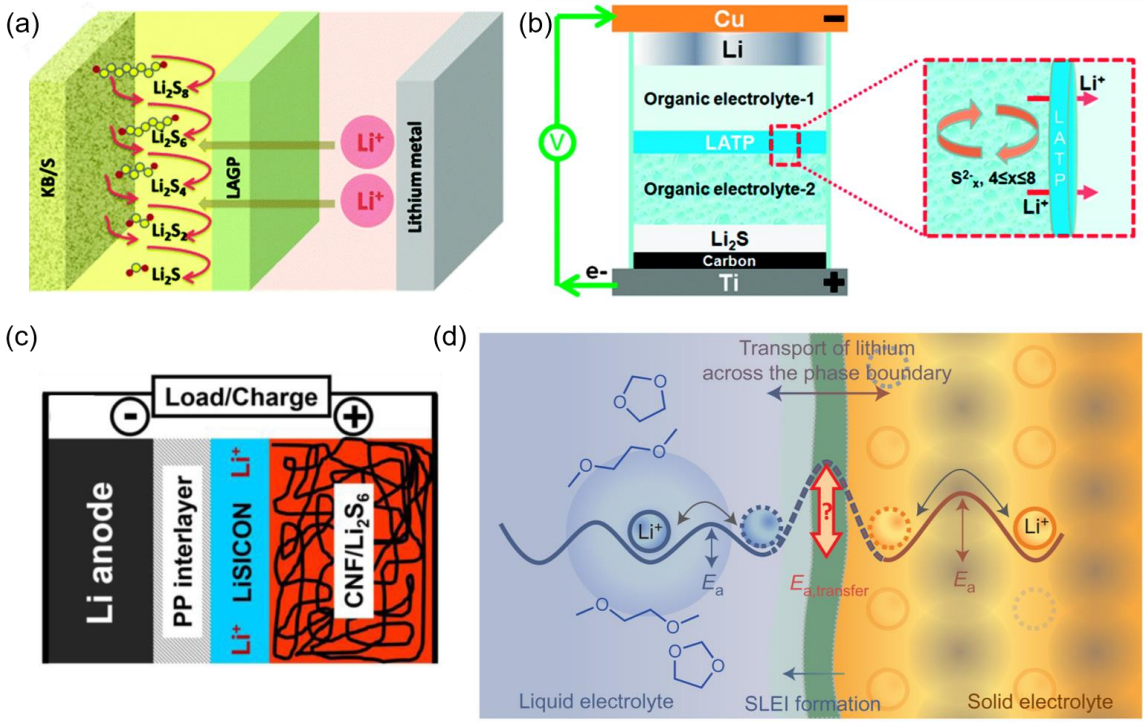

Figure 19. Liquid-solid hybrid electrolytes for Li metal batteries. a) Schematic of a hybrid Li–S cell using LAGP solid electrolyte. Reproduced with permission.[102b] Copyright 2014, Royal Society of Chemistry. b) Schematic of a hybrid Li-Li_2S cell using LISICON type LATP solid electrolyte. Reproduced with permission.[102c] Copyright 2015, Royal Society of Chemistry. c) Schematic of a hybrid Li-Li_2S_6 cell using LISICON type LATP solid electrolyte. Reproduced with permission.[102d] Copyright 2015, American Chemical Society. d) Schematic of ion transport at the interface of liquid electrolyte and solid electrolyte. Reproduced with permission.[102e] Copyright 2015, American Chemical Society.

4. Conclusions and perspective

Li metal batteries have been considered as the "Holy Grail" of battery anodes and have attracted extensive research for decades. Despite persistent efforts to develop safe and high-performance Li metal batteries, the intrinsic instability of Li metal in organic electrolytes and dendritic deposition nature of Li metal remain challenging. Recent research interest has been devoted to electrolyte modification, interface protection, and electrode framework construction. Seizing the opportunity to use the nanotechnology, strategies such as nano-engineering at interfaces and constructing nanostructured frameworks for Li metal anodes have remarkably stimulated the development of Li metal batteries. However, current research is usually focused on partial problems of Li metal anode, suppressing the dendrite problems or improving the Coulombic efficiency. For example, although some approaches have been reported effective to mitigate the growth of Li dendrites, the Li metal anodes were cycled at low current densities (typically 0.5-1 mA cm^{-2}) with low areal capacities (~1 mA h cm^{-2}) and low Coulombic efficiencies (~95%), which cannot meet the requirement in practical full batteries. Improving the Coulombic efficiency of the Li metal anode to greater than 99.5% could be more challenging. To realize a dendrite-free and highly reversible Li metal battery, it is crucial to resolve all issues of the Li metal anode. This could not be accomplished unless comprehensive treatments are adopted, which will combine modification of the Li electrode, the organic electrolyte and additives, the Li metal interfaces, the separator, and the battery configuration. It will require more efforts on the Li anode study but it is deserved considering the wide range of applications for high-energy Li metal batteries.

Solid-state batteries are expected to hold higher energy density and better safety than the liquid batteries. With high mechanical strength and Li-ion transfer number, SSEs are ideal candidates to address the problems of Li metal anodes in the organic electrolytes. As depicted in **Figure 20**, the evolution trend of the battery is from liquid batteries to solid-state batteries with energy density and safety advantages. However, the interfacial instability and impedance

of the SSEs with both electrodes as well as other problems discussed above have hindered the utility of solid-state batteries.

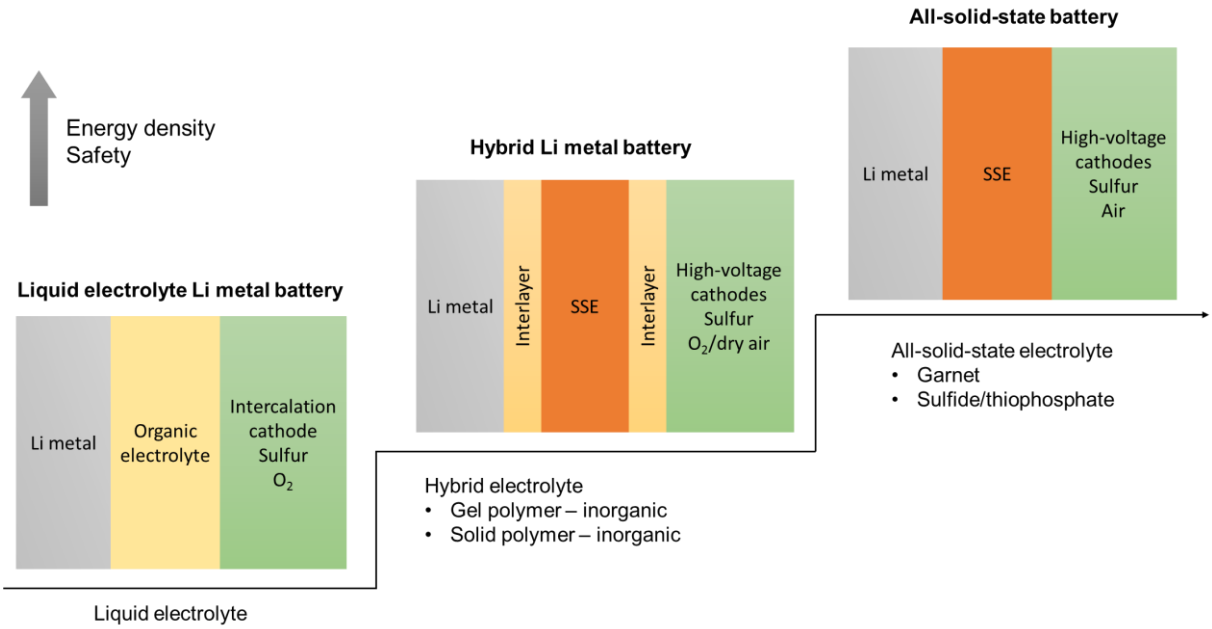

Figure 20. Development of Li metal batteries from the liquid electrolyte battery to the polymer-inorganic hybrid battery, and finally all-solid-state battery. The all-solid-state battery is expected to hold higher energy density and safety.

To address challenges of interfaces between SSEs and electrodes will be one of the main research interests. Employing interlayers such as gel polymers and solid polymers (as illustrated in Figure 20) can be an effective way reduce interfacial resistance and prevent side reactions between SSE and the Li metal. The interlayer should have a high ionic conductivity at room temperature, wide thermal stability, and good chemical compatibility with solid electrolytes and electrodes. Therefore, hybrid Li metal batteries will strongly rely on the interlayer to function properly at room temperature.

To build a solid electrolyte framework will be another research interest. A solid electrolyte framework can host electrodes and physically confine Li metal and cathode materials, to prevent potential volume change during Li cycling. The design of binary solid electrolytes will make it possible to improve both ionic conductivity at room temperature and chemical

stability against electrodes. For example, sulfide electrolyte holds a superior high ionic conductivity but a poor stability with Li; oxide garnet electrolyte has a stable interface with Li metal but a relatively low ionic conductivity (~10^{-4} S cm^{-1}) at room temperature. A binary electrolyte based on sulfate and oxide garnet could exhibit balanced properties in ionic conductivity and chemical stability. To develop a high-performance solid-state Li metal battery with high safety will be the ultimate goal for battery development. Solid-state Li metal batteries are expected to address challenges in conventional Li-S and Li-air batteries and will bring new opportunity to develop advanced Li metal batteries with a high energy density and reliable safety.

Acknowledgements

This work was supported by the US Department of Energy ARPA-E (Contract No. DE-AR0000384) and EERE (Contract No. DE-EE0006860). This work was supported as part of the Nanostructures for Electrical Energy Storage (NEES), an Energy Frontier Research Center funded by the US Department of Energy, Office of Science, and Basic Energy Sciences under Award number DESC0001160. Y. Zhang would like to acknowledge the China Scholarship Council (CSC No. 201506680044) for financial support. The authors thank Yudi Kuang for the help with the figures. C. Yang and K. Fu contributed equally to this work.

Received: ((will be filled in by the editorial staff))
Revised: ((will be filled in by the editorial staff))
Published online: ((will be filled in by the editorial staff))

References

[1] a) M. Armand, J.-M. Tarascon, *Nature* **2008**, *451*, 652; b) J. B. Goodenough, Y. Kim, *Chem. Mater.* **2010**, *22*, 587.

[2] P. G. Bruce, S. A. Freunberger, L. J. Hardwick, J. M. Tarascon, *Nat. Mater.* **2012**, *11*, 19.

[3] W. Xu, J. Wang, F. Ding, X. Chen, E. Nasybulin, Y. Zhang, J.-G. Zhang, *Energy Environ. Sci.* **2014**, *7*, 513.

[4] J. M. Tarascon, M. Armand, *Nature* **2001**, *414*, 359.

[5] D. Aurbach, E. Zinigrad, Y. Cohen, H. Teller, *Solid State Ionics* **2002**, *148*, 405.

[6] A. Manthiram, X. Yu, S. Wang, *Nat. Rev. Mater.* **2017**, *2*, 16103.

[7] H. Kim, G. Jeong, Y.-U. Kim, J.-H. Kim, C.-M. Park, H.-J. Sohn, *Chem. Soc. Rev.* **2013**, *42*, 9011.

[8] a) D. Aurbach, Y. Gofer, M. Ben-Zion, P. Aped, *J. Electroanal. Chem.* **1992**, *339*, 451; b) D. Aurbach, A. Zaban, Y. Gofer, Y. E. Ely, I. Weissman, O. Chusid, O. Abramson, *J. Power Sources* **1995**, *54*, 76.

[9] a) D. Lu, Y. Shao, T. Lozano, W. D. Bennett, G. L. Graff, B. Polzin, J. Zhang, M. H. Engelhard, N. T. Saenz, W. A. Henderson, P. Bhattacharya, J. Liu, J. Xiao, *Adv. Energy Mater.* **2015**, *5*, 1400993; b) K. N. Wood, E. Kazyak, A. F. Chadwick, K.-H. Chen, J.-G. Zhang, K. Thornton, N. P. Dasgupta, *ACS Cent. Sci.* **2016**, *2*, 790.

[10] X. B. Cheng, R. Zhang, C. Z. Zhao, F. Wei, J. G. Zhang, Q. Zhang, *Adv. Sci.* **2016**, *3*, 1500213.

[11] K. Xu, *Chem. Rev.* **2004**, *104*, 4303.

[12] a) S. A. Freunberger, Y. Chen, Z. Peng, J. M. Griffin, L. J. Hardwick, F. Bardé, P. Novák, P. G. Bruce, *J. Am. Chem. Soc.* **2011**, *133*, 8040; b) J. Gao, M. A. Lowe, Y. Kiya, H. D. Abruña, *J. Phys. Chem. C* **2011**, *115*, 25132.

[13] a) D. Xu, Z. L. Wang, J. J. Xu, L. L. Zhang, X. B. Zhang, *Chem. Commun.* **2012**, *48*, 6948; b) X. Ji, K. Lee, L. F. Nazar, *Nat. Mater.* **2009**, *8*, 500; c) L. Johnson, C. Li, Z. Liu, Y. Chen, S. A. Freunberger, P. C. Ashok, B. B. Praveen, K. Dholakia, J.-M. Tarascon, P. G. Bruce, *Nat. Chem.* **2014**, *6*, 1091.

[14] D. R. MacFarlane, M. Forsyth, P. C. Howlett, J. M. Pringle, J. Sun, G. Annat, W. Neil, E. I. Izgorodina, *Acc. Chem. Res.* **2007**, *40*, 1165.

[15] A. Eftekhari, Y. Liu, P. Chen, *J. Power Sources* **2016**, *334*, 221.

[16] M. Armand, F. Endres, D. R. MacFarlane, H. Ohno, B. Scrosati, *Nat. Mater.* **2009**, *8*, 621.

[17] Y. Lu, S. K. Das, S. S. Moganty, L. A. Archer, *Adv. Mater.* **2012**, *24*, 4430.

[18] Y. Lu, K. Korf, Y. Kambe, Z. Tu, L. A. Archer, *Angew. Chem. Int. Ed.* **2014**, *53*, 488.

[19] N. W. Li, Y. X. Yin, J. Y. Li, C. H. Zhang, Y. G. Guo, *Adv. Sci.* **2017**, *4*, 1600400.

[20] a) A. Zaban, D. Aurbach, *J. Power Sources* **1995**, *54*, 289; b) D. Aurbach, E. Zinigrad, H. Teller, P. Dan, *J. Electrochem. Soc.* **2000**, *147*, 1274.

[21] a) J. J. Hu, G. K. Long, S. Liu, G. R. Li, X. P. Gao, *Chem. Commun.* **2014**, *50*, 14647; b) R. Miao, J. Yang, X. Feng, H. Jia, J. Wang, Y. Nuli, *J. Power Sources* **2014**, *271*, 291.

[22] D. Aurbach, A. Zaban, *J. Electroanal. Chem.* **1993**, *348*, 155.

[23] J. Qian, W. A. Henderson, W. Xu, P. Bhattacharya, M. Engelhard, O. Borodin, J.-G. Zhang, *Nat. Commun.* **2015**, *6*, 6362.

[24] L. Suo, Y.-S. S. Hu, H. Li, M. Armand, L. Chen, *Nat. Commun.* **2013**, *4*, 1481.

[25] S. Shiraishi, K. Kanamura, Z. i. Takehara, *J. Electrochem. Soc.* **1999**, *146*, 1633.

[26] J. K. Stark, Y. Ding, P. A. Kohl, *J. Electrochem. Soc.* **2011**, *158*, A1100.

[27] a) X.-Q. Zhang, X.-B. Cheng, X. Chen, C. Yan, Q. Zhang, *Adv. Funct. Mater.* **2017**, DOI: 10.1002/adfm.201605989; b) R. Mogi, M. Inaba, S.-K. Jeong, Y. Iriyama, T. Abe, Z. Ogumi, *J. Electrochem. Soc.* **2002**, *149*, A1578.

[28] M. Morita, S. Aoki, Y. Matsuda, *Electrochim. Acta* **1992**, *37*, 119.

[29] a) J. A. Vega, J. Zhou, P. A. Kohl, *J. Electrochem. Soc.* **2009**, *156*, A253; b) M. Ishikawa, S. Yoshitake, M. Morita, Y. Matsuda, *J. Electrochem. Soc.* **1994**, *141*, L159.

[30] K. Saito, Y. Nemoto, S. Tobishima, J. Yamaki, *J. Power Sources* **1997**, *68*, 476.

[31] S. S. Zhang, *Electrochim. Acta* **2012**, *70*, 344.

[32] a) S. Xiong, K. Xie, Y. Diao, X. Hong, *J. Power Sources* **2014**, *246*, 840; b) W. Li, H. Yao, K. Yan, G. Zheng, Z. Liang, Y.-M. Chiang, Y. Cui, *Nat. Commun.* **2015**, *6*, 7436; c) C. Yan, X.-B. Cheng, C.-Z. Zhao, J.-Q. Huang, S.-T. Yang, Q. Zhang, *J. Power Sources* **2016**, *327*, 212.

[33] C.-Z. Zhao, X.-B. Cheng, R. Zhang, H.-J. Peng, J.-Q. Huang, R. Ran, Z.-H. Huang, F. Wei, Q. Zhang, *Energy Storage Mater.* **2016**, *3*, 77.

[34] F. Ding, W. Xu, G. L. Graff, J. Zhang, M. L. Sushko, X. Chen, Y. Shao, M. H. Engelhard, Z. Nie, J. Xiao, X. Liu, P. V. Sushko, J. Liu, J.-G. Zhang, *J. Am. Chem. Soc.* **2013**, *135*, 4450.

[35] Y. Zhang, J. Qian, W. Xu, S. M. Russell, X. Chen, E. Nasybulin, P. Bhattacharya, M. H. Engelhard, D. Mei, R. Cao, F. Ding, A. V. Cresce, K. Xu, J.-G. Zhang, *Nano Lett.* **2014**, *14*, 6889.

[36] a) F. Wu, J. Qian, R. Chen, J. Lu, L. Li, H. Wu, J. Chen, T. Zhao, Y. Ye, K. Amine, *ACS Appl. Mater. Interfaces* **2014**, *6*, 15542; b) W. Jia, C. Fan, L. Wang, Q. Wang, M. Zhao, A. Zhou, J. Li, *ACS Appl. Mater. Interfaces* **2016**, *8*, 15399.

[37] Y. Lu, Z. Tu, L. A. Archer, *Nat. Mater.* **2014**, *13*, 961.

[38] a) J. Qian, W. Xu, P. Bhattacharya, M. Engelhard, W. A. Henderson, Y. Zhang, J.-G. Zhang, *Nano Energy* **2015**, *15*, 135; b) N. Togasaki, T. Momma, T. Osaka, *J. Power Sources* **2014**, *261*, 23.

[39] a) H. Jia, J. Wang, F. Lin, C. W. Monroe, J. Yang, Y. NuLi, *Chem. Commun.* **2014**, *50*, 7011; b) J. Wang, F. Lin, H. Jia, J. Yang, C. W. Monroe, Y. NuLi, *Angew. Chem. Int. Ed.* **2014**, *53*, 10099.

[40] N. W. Li, Y. X. Yin, C. P. Yang, Y. G. Guo, *Adv. Mater.* **2016**, *28*, 1853.

[41] a) C. Monroe, J. Newman, *J. Electrochem. Soc.* **2005**, *152*, A396; b) G. M. Stone, S. A. Mullin, A. A. Teran, D. T. Hallinan, A. M. Minor, A. Hexemer, N. P. Balsara, *J. Electrochem. Soc.* **2012**, *159*, A222.

[42] L. Wang, Q. Wang, W. Jia, S. Chen, P. Gao, J. Li, *J. Power Sources* **2017**, *342*, 175.

[43] A. Basile, A. I. Bhatt, A. P. O'Mullane, *Nat. Commun.* **2016**, *7*, 11794.

[44] G. A. Umeda, E. Menke, M. Richard, K. L. Stamm, F. Wudl, B. Dunn, *J. Mater. Chem.* **2011**, *21*, 1593.

[45] a) M. Wu, Z. Wen, Y. Liu, X. Wang, L. Huang, *J. Power Sources* **2011**, *196*, 8091; b) G. Ma, Z. Wen, M. Wu, C. Shen, Q. Wang, J. Jin, X. Wu, *Chem. Commun.* **2014**, *50*, 14209.

[46] M. Wu, Z. Wen, J. Jin, B. V. R. Chowdari, *ACS Appl. Mater. Interfaces* **2016**, *8*, 16386.

[47] a) Q. C. Liu, J. J. Xu, S. Yuan, Z. W. Chang, D. Xu, Y. B. Yin, L. Li, H. X. Zhong, Y. S. Jiang, J. M. Yan, X. B. Zhang, *Adv. Mater.* **2015**, *27*, 5241; b) X.-B. Cheng, C. Yan, X. Chen, C. Guan, J.-Q. Huang, H.-J. Peng, R. Zhang, S.-T. Yang, Q. Zhang, *Chem* **2017**, *2*, 258.

[48] a) A. C. Kozen, C. F. Lin, A. J. Pearse, M. A. Schroeder, X. Han, L. Hu, S. B. Lee, G. W. Rubloff, M. Noked, *ACS Nano* **2015**, *9*, 5884; b) E. Kazyak, K. N. Wood, N. P. Dasgupta, *Chem. Mater.* **2015**, *27*, 6457; c) Y. Cao, X. Meng, J. W. Elam, *ChemElectroChem* **2016**, *3*, 858.

[49] K. Yan, H.-W. Lee, T. Gao, G. Zheng, H. Yao, H. Wang, Z. Lu, Y. Zhou, Z. Liang, Z. Liu, S. Chu, Y. Cui, *Nano Lett.* **2014**, *14*, 6016.

[50] G. Zheng, C. Wang, A. Pei, J. Lopez, F. Shi, Z. Chen, A. D. Sendek, H.-W. Lee, Z. Lu, H. Schneider, M. M. Safont-Sempere, S. Chu, Z. Bao, Y. Cui, *ACS Energy Lett.* **2016**, *1*, 1247.

[51] W. Liu, D. Lin, A. Pei, Y. Cui, *J. Am. Chem. Soc.* **2016**, *138*, 15443.

[52] R. Zhang, N.-W. Li, X.-B. Cheng, Y.-X. Yin, Q. Zhang, Y.-G. Guo, *Adv. Sci.* **2017**, DOI: 10.1002/advs.201600445.

[53] X.-B. Cheng, T.-Z. Hou, R. Zhang, H.-J. Peng, C.-Z. Zhao, J.-Q. Huang, Q. Zhang, *Adv. Mater.* **2016**, *28*, 2888.

[54] P. Bai, J. Li, F. R. Brushett, M. Z. Bazant, *Energy Environ. Sci.* **2016**, *9*, 3221.

[55] B. Zhu, Y. Jin, X. Hu, Q. Zheng, S. Zhang, Q. Wang, J. Zhu, *Adv. Mater.* **2016**, *29*, 1603755.

[56] Y. Liu, D. Lin, P. Y. Yuen, K. Liu, J. Xie, R. H. Dauskardt, Y. Cui, *Adv. Mater.* **2017**, DOI: 10.1002/adma.201605531.

[57] C. Yang, B. Liu, F. Jiang, Y. Zhang, H. Xie, E. Hitz, L. Hu, *Nano Res.* **2017**, DOI: 10.1007/s12274-017-1498-2.

[58] Y. Wang, P. He, H. Zhou, *Energy Environ. Sci.* **2011**, *4*, 4994.

[59] X. Wang, Y. Hou, Y. Zhu, Y. Wu, R. Holze, *Sci. Rep.* **2013**, *3*, 1401.

[60] X. Ji, D. Y. Liu, D. G. Prendiville, Y. Zhang, X. Liu, G. D. Stucky, *Nano Today* **2012**, *7*, 10.

[61] R. Zhang, X. B. Cheng, C. Z. Zhao, H. J. Peng, J. L. Shi, J. Q. Huang, J. Wang, F. Wei, Q. Zhang, *Adv. Mater.* **2016**, *28*, 2155.

[62] a) Y. Sun, G. Zheng, Z. W. Seh, N. Liu, S. Wang, J. Sun, H. R. Lee, Y. Cui, *Chem* **2016**, *1*, 287; b) S. Jin, S. Xin, L. Wang, Z. Du, L. Cao, J. Chen, X. Kong, M. Gong, J. Lu, Y. Zhu, H. Ji, R. S. Ruoff, *Adv. Mater.* **2016**, *28*, 9094.

[63] K. Yan, Z. Lu, H.-W. Lee, F. Xiong, P.-C. Hsu, Y. Li, J. Zhao, S. Chu, Y. Cui, *Nat. Energy* **2016**, *1*, 16010.

[64] X. Gui, J. Wei, K. Wang, A. Cao, H. Zhu, Y. Jia, Q. Shu, D. Wu, *Adv. Mater.* **2010**, *22*, 617.

[65] Y. Zhang, B. Liu, E. Hitz, W. Luo, Y. Yao, Y. Li, J. Dai, C. Chen, Y. Wang, C. Yang, H. Li, L. Hu, *Nano Res.* **2017**, DOI: 10.1007/s12274-017-1461-2.

[66] a) X. B. Cheng, H. J. Peng, J. Q. Huang, F. Wei, Q. Zhang, *Small* **2014**, *10*, 4257; b) X. Zhang, W. Wang, A. Wang, Y. Huang, K. Yuan, Z. Yu, J. Qiu, Y. Yang, *J. Mater. Chem. A* **2014**, *2*, 11660.

[67] C.-P. Yang, Y.-X. Yin, S.-F. Zhang, N.-W. Li, Y.-G. Guo, *Nat. Commun.* **2015**, *6*, 8058.

[68] Q. Yun, Y.-B. He, W. Lv, Y. Zhao, B. Li, F. Kang, Q.-H. Yang, *Adv. Mater.* **2016**, *28*, 6932.

[69] L.-L. Lu, J. Ge, J.-N. Yang, S.-M. Chen, H. Yao, F. Zhou, S.-H. Yu, *Nano Lett.* **2016**, *16*, 4431.

[70] Z. Zhang, X. Xu, S. Wang, Z. Peng, M. Liu, J. Zhou, C. Shen, D. Wang, *ACS Appl. Mater. Interfaces* **2016**, *8*, 26801.

[71] a) Z. Liang, D. Lin, J. Zhao, Z. Lu, Y. Liu, C. Liu, Y. Lu, H. Wang, K. Yan, X. Tao, *Proc. Natl. Acad. Sci.* **2016**, *113*, 2862; b) Y. Zhang, W. Luo, C. Wang, Y. Li, C. Chen, J. Song, J. Dai, M. E. Hitz, S. Xu, C. Yang, Y. Wang, L. Hu, *Proc. Natl. Acad. Sci.* **2017**, DOI: 10.1073/pnas.1618871114; c) Y. Liu, D. Lin, Z. Liang, J. Zhao, K. Yan, Y. Cui, *Nat. Commun.* **2016**, *7*, 10992; d) D. Lin, Y. Liu, Z. Liang, H.-W. Lee, J. Sun, H. Wang, K. Yan, J. Xie, Y. Cui, *Nat. Nanotech.* **2016**, *11*, 626.

[72] a) P. Arora, Z. Zhang, *Chem. Rev.* **2004**, *104*, 4419; b) S. S. Zhang, *J. Power Sources* **2007**, *164*, 351; c) S. M. Kang, M.-H. Ryou, J. W. Choi, H. Lee, *Chem. Mater.* **2012**, *24*, 3481; d) J.-H. Park, J.-H. Cho, W. Park, D. Ryoo, S.-J. Yoon, J. H. Kim, Y. U. Jeong, S.-Y. Lee, *J. Power Sources* **2010**, *195*, 8306; e) W.-K. Shin, A. G. Kannan, D.-W. Kim, *ACS Appl. Mater. Interfaces* **2015**, *7*, 23700.

[73] K. Liu, D. Zhuo, H. W. Lee, W. Liu, D. Lin, Y. Lu, Y. Cui, *Adv. Mater.* **2017**, *29*, 1603987.

[74] W. Luo, L. Zhou, K. Fu, Z. Yang, J. Wan, M. Manno, Y. Yao, H. Zhu, B. Yang, L. Hu, *Nano Lett.* **2015**, *15*, 6149.

[75] a) H. Wu, D. Zhuo, D. Kong, Y. Cui, *Nat. Commun.* **2014**, *5*, 5193; b) D. Lin, D. Zhuo, Y. Liu, Y. Cui, *J. Am. Chem. Soc.* **2016**, *138*, 11044.

[76] J. Janek, W. G. Zeier, *Nat. Energy* **2016**, *1*, 16141.

[77] a) Y. Seino, T. Ota, K. Takada, A. Hayashi, M. Tatsumisago, *Energy Environ. Sci.* **2014**, *7*, 627; b) R. Murugan, V. Thangadurai, W. Weppner, *Angew. Chem. Int. Ed.* **2007**, *46*, 7778; c) V. Thangadurai, S. Narayanan, D. Pinzaru, *Chem. Soc. Rev.* **2014**, *43*, 4714.

[78] a) R. Bouchet, S. Maria, R. Meziane, A. Aboulaich, L. Lienafa, J.-P. Bonnet, T. N. T. Phan, D. Bertin, D. Gigmes, D. Devaux, R. Denoyel, M. Armand, *Nat. Mater.* **2013**, *12*, 452; b) S.-O. Tung, S. Ho, M. Yang, R. Zhang, N. A. Kotov, *Nat. Commun.* **2015**, *6*, 6152.

[79] Z. Tu, Y. Kambe, Y. Lu, L. A. Archer, *Adv. Energy Mater.* **2014**, *4*, 1300654.

[80] D. Zhou, R. Liu, Y.-B. He, F. Li, M. Liu, B. Li, Q.-H. Yang, Q. Cai, F. Kang, *Adv. Energy Mater.* **2016**, *6*, 1502214.

[81] a) D. Lee, H. Lee, Y. J. Kim, J. K. Park, H. T. Kim, *Adv. Mater.* **2016**, *28*, 857; b) H. Lee, D. Lee, Y.-J. Kim, J.-K. Park, H.-T. Kim, *J. Power Sources* **2015**, *284*, 103.

[82] Q. Lu, Y. B. He, Q. Yu, B. Li, Y. Kaneti, Y. Yao, F. Kang, Q. H. Yang, *Adv. Mater.* **2017**, DOI: 10.1002/adma.201604460.

[83] a) Z. Xue, D. He, X. Xie, *J. Mater. Chem. A* **2015**, *3*, 19218; b) L. Yue, J. Ma, J. Zhang, J. Zhao, S. Dong, Z. Liu, G. Cui, L. Chen, *Energy Storage Mater.* **2016**, *5*, 139.

[84] M. D. Tikekar, S. Choudhury, Z. Tu, L. A. Archer, *Nat. Energy* **2016**, *1*, 16114.

[85] R. Khurana, J. L. Schaefer, L. A. Archer, G. W. Coates, *J. Am. Chem. Soc.* **2014**, *136*, 7395.

[86] Q. Pan, D. M. Smith, H. Qi, S. Wang, C. Y. Li, *Adv. Mater.* **2015**, *27*, 5995.

[87] a) W. Zhou, H. Gao, J. B. Goodenough, *Adv. Energy Mater.* **2016**, *6*, 1501802; b) Y.-J. Wang, Y. Pan, D. Kim, *J. Power Sources* **2006**, *159*, 690; c) D. Lin, W. Liu, Y. Liu, H. Lee, P.-C. Hsu, K. Liu, Y. Cui, *Nano Lett.* **2016**, *16*, 459; d) S. Liu, N. Imanishi, T. Zhang, A. Hirano, Y. Takeda, O. Yamamoto, J. Yang, *J. Power Sources* **2010**, *195*, 6847; e) I. Gurevitch,

R. Buonsanti, A. A. Teran, B. Gludovatz, R. O. Ritchie, J. Cabana, N. P. Balsara, *J. Electrochem. Soc.* **2013**, *160*, A1611; f) L. Damen, J. Hassoun, M. Mastragostino, B. Scrosati, *J. Power Sources* **2010**, *195*, 6902; g) F. Croce, G. B. Appetecchi, L. Persi, B. Scrosati, *Nature* **1998**, *394*, 456; h) J. H. Choi, C. H. Lee, J. H. Yu, C. H. Doh, S. M. Lee, *J. Power Sources* **2015**, *274*, 458; i) J. Zhang, N. Zhao, M. Zhang, Y. Li, P. K. Chu, X. Guo, Z. Di, X. Wang, H. Li, *Nano Energy* **2016**, *28*, 447.

[88] W. Wang, E. Yi, A. J. Fici, R. M. Laine, J. Kieffer, *J. Phys. Chem. C* **2017**, *121*, 2563.

[89] W. Liu, N. Liu, J. Sun, P. C. Hsu, Y. Li, H. W. Lee, Y. Cui, *Nano Lett.* **2015**, *15*, 2740.

[90] W. Liu, D. Lin, J. Sun, G. Zhou, Y. Cui, *ACS Nano* **2016**, *10*, 11407.

[91] K. K. Fu, Y. Gong, J. Dai, A. Gong, X. Han, Y. Yao, C. Wang, Y. Wang, Y. Chen, C. Yan, Y. Li, E. D. Wachsman, L. Hu, *Proc. Natl. Acad. Sci.* **2016**, *113*, 7094.

[92] Y. Zhu, X. He, Y. Mo, *ACS Appl. Mater. Interfaces* **2015**, *7*, 23685.

[93] F. Han, Y. Zhu, X. He, Y. Mo, C. Wang, *Adv. Energy Mater.* **2016**, *6*, 1501590.

[94] a) G. Sahu, E. Rangasamy, J. Li, Y. Chen, K. An, N. Dudney, C. Liang, *J. Mater. Chem. A* **2014**, *2*, 10396; b) E. Rangasamy, G. Sahu, J. K. Keum, A. J. Rondinone, N. J. Dudney, C. Liang, *J. Mater. Chem. A* **2014**, *2*, 4111; c) D. Þ. Sveinbjörnsson, T. Vegge, P. Norby, M. B. Mogensen, *Ph.D. Thesis*, Technical University of Denmark, **2014**.

[95] a) S. Ohta, T. Kobayashi, T. Asaoka, *J. Power Sources* **2011**, *196*, 3342; b) H. Buschmann, S. Berendts, B. Mogwitz, J. Janek, *J. Power Sources* **2012**, *206*, 236; c) K. Tadanaga, R. Takano, T. Ichinose, S. Mori, A. Hayashi, M. Tatsumisago, *Electrochem. Commun.* **2013**, *33*, 51; d) S. Narayanan, G. T. Hitz, E. D. Wachsman, V. Thangadurai, *J. Electrochem. Soc.* **2015**, *162*, 1772; e) X. Tong, V. Thangadurai, E. D. Wachsman, *Inorg. Chem.* **2015**, *54*, 3600; f) Y. Kim, A. Yoo, R. Schmidt, A. Sharafi, H. Lee, J. Wolfenstine, J. Sakamoto, *Front. Energy Res.* **2016**, *4*, 1; g) M. Kotobuki, H. Munakata, K. Kanamura, Y. Sato, T. Yoshida, *J. Electrochem. Soc.* **2010**, *157*, A1076; h) K. Ishiguro, Y. Nakata, M.

Matsui, I. Uechi, Y. Takeda, O. Yamamoto, N. Imanishi, *J. Electrochem. Soc.* **2013**, *160*, A1690; i) R. H. Basappa, T. Ito, H. Yamada, *J. Electrochem. Soc.* **2017**, *164*, A666.

[96] A. C. Luntz, J. Voss, K. Reuter, *J. Phys. Chem. Lett.* **2015**, *6*, 4599.

[97] a) R. Sudo, Y. Nakata, K. Ishiguro, M. Matsui, A. Hirano, Y. Takeda, O. Yamamoto, N. Imanishi, *Solid State Ionics* **2014**, *262*, 151; b) L. Cheng, W. Chen, M. Kunz, K. Persson, N. Tamura, G. Chen, M. Doeff, *ACS Appl. Mater. Interfaces* **2015**, *7*, 2073.

[98] X. Han, Y. Gong, K. Fu, X. He, G. T. Hitz, J. Dai, A. Pearse, B. Liu, H. Wang, G. Rubloff, Y. Mo, V. Thangadurai, E. D. Wachsman, L. Hu, *Nat. Mater.* **2017**, DOI: 10.1038/nmat4821.

[99] a) C. L. Tsai, V. Roddatis, C. V. Chandran, Q. Ma, S. Uhlenbruck, M. Bram, P. Heitjans, O. Guillon, *ACS Appl. Mater. Interfaces* **2016**, *8*, 10617; b) W. Luo, Y. Gong, Y. Zhu, K. K. Fu, J. Dai, S. D. Lacey, C. Wang, B. Liu, X. Han, Y. Mo, E. D. Wachsman, L. Hu, *J. Am. Chem. Soc.* **2016**, *138*, 12258; c) C. Wang, Y. Gong, B. Liu, K. Fu, Y. Yao, E. Hitz, Y. Li, J. Dai, S. Xu, W. Luo, E. D. Wachsman, L. Hu, *Nano Lett.* **2017**, *17*, 565.

[100] J. van den Broek, S. Afyon, J. L. M. Rupp, *Adv. Energy Mater.* **2016**, *6*, 1600736.

[101] a) Y. Li, B. Xu, H. Xu, H. Duan, X. Lü, S. Xin, W. Zhou, L. Xue, G. Fu, A. Manthiram, J. B. Goodenough, *Angew. Chem. Int. Ed.* **2017**, *56*, 753; b) W. Zhou, Y. Li, S. Xin, J. B. Goodenough, *ACS Cent. Sci.* **2017**, *3*, 52; c) Y. Li, W. Zhou, X. Chen, X. Lü, Z. Cui, S. Xin, L. Xue, Q. Jia, J. B. Goodenough, *Proc. Natl. Acad. Sci.* **2016**, *113*, 13313; d) W. Zhou, S. Wang, Y. Li, S. Xin, A. Manthiram, J. B. Goodenough, *J. Am. Chem. Soc.* **2016**, *138*, 9385.

[102] a) M. Hagen, S. Dorfler, H. Althues, J. Tubke, M. J. Hoffmann, S. Kaskel, K. Pinkwart, *J. Power Sources* **2012**, *213*, 239; b) Q. Wang, J. Jin, X. Wu, G. Ma, J. Yang, Z. Wen, *Phys. Chem. Chem. Phys.* **2014**, *16*, 21225; c) L. Wang, Y. Wang, Y. Xia, *Energy Environ. Sci.* **2015**, *8*, 1551; d) X. Yu, Z. Bi, F. Zhao, A. Manthiram, *ACS Appl. Mater. Interfaces* **2015**, *7*, 16625; e) M. R. Busche, T. Drossel, T. Leichtweiss, D. A. Weber, M. Falk,

M. Schneider, M.-l. Reich, H. Sommer, P. Adelhelm, J. Janek, *Nat. Chem.* **2016**, *8*, 426; f) H. Kitaura, H. Zhou, *Sci. Rep.* **2015**, *5*, 13271.

Lithium metal batteries are promising candidates for the high-energy and cost-effective energy storage systems. Solving the dendritic problem and interfacial instability of the Li metal anodes is a prerequisite to their practical utilization. This paper reviews strategies to protect Li metal anodes in liquid and solid-state electrolytes, which will facilitate the development safe and high-performance Li metal batteries.

Keyword: Electrochemical energy storage, Li metal battery, Li dendrite, organic electrolyte, solid-state electrolyte

Chunpeng Yang[†], Kun (Kelvin) Fu[†], Ying Zhang, Emily Hitz, and Liangbing Hu[*]

Protected Lithium Metal Anode in Batteries: From Liquid to Solid
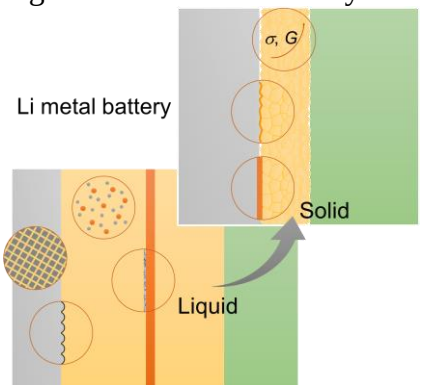
ToC figure ((Please choose one size: 55 mm broad × 50 mm high **or** 110 mm broad × 20 mm high. Please do not use any other dimensions))